Cell Biology

Neuropilin-1 controls vascular permeability through juxtacrine regulation of endothelial adherens junctions

Sagnik Pal, Yangyang Su, Lena Claesson-Welsh, Mark Richards

Dept. of Immunology, Genetics and Pathology, Beijer and Science for Life Laboratories, Uppsala University, Uppsala, Sweden

Reviewed Preprint

Published from the original preprint after peer review and assessment by eLife.

About eLife's process

Reviewed preprint version 1
April 11, 2024 (this version)

Posted to preprint server
January 24, 2024

Sent for peer review
January 23, 2024

Abstract

Neuropilin-1 (NRP1) regulates endothelial cell (EC) biology through modulating vascular endothelial growth factor receptor 2 (VEGFR2) signalling by presenting VEGFA. How NRP1 impacts VEGFA-mediated vascular hyperpermeability however is unresolved, being described as having a positive or passive function. Using EC-specific *Nrp1* knock-out mice, we discover that EC-expressed NRP1 exerts an organotypic role. In ear skin, VEGFA/VEGFR2-mediated vascular leakage increased following EC NRP1 knock-out, showing that NRP1 negatively regulates VEGFR2 signalling. Conversely, in back skin and trachea, EC NRP1 knock-out decreased vascular leakage. Accordingly, VE-cadherin phosphorylation increased in the ear skin but was suppressed in back skin of *Nrp1* iECKO mice. NRP1 has been shown to have the ability to act in a juxtacrine manner. Importantly, NRP1 was more abundant in perivascular cells of the ear skin than back skin. Global NRP1 knock-out suppressed VEGFA-induced vascular leakage in the ear skin, implicating perivascular NRP1 as a juxtacrine co-receptor of VEGFA in this compartment. Altogether, we demonstrate that perivascular NRP1 is an active participant in EC VEGFA/VEGFR2 signalling and acts as an organotypic modifier of EC biology.

eLife assessment

This study is focused on the question of how Nrp1 contributes to the regulation of vascular permeability and whether or why there are differences between different vascular beds. The scientific concept of this paper suggests a possible role of Nrp1 on perivascular cells as a participant in the regulation of vascular permeability. This concept is interesting and potentially **useful**. However, the methodology and quantitative analysis are currently **inadequate** to fully support the claims.

Introduction

Neuropilin 1 (NRP1) is a multifunctional transmembrane protein that is expressed abundantly on the surface of a range cell types, where it binds class 3 semaphorins (SEMA3), heparan sulfate and vascular endothelial growth factors (VEGFs) (Goshima et al., 1999, Mamluk et al., 2002, Gu et al., 2002). VEGFA is the main activator of VEGF receptor 2 (VEGFR2) signalling in endothelial cells (ECs) and its binding to NRP1 promotes heterocomplex formation between NRP1 and VEGFR2 (Soker et al., 2002). Thus, NRP1 has been designated as a co-receptor of VEGFR2 and is known to modulate VEGFR2 signalling. The cytoplasmic domain of NRP1 contains a C-terminal SEA motif, a PDZ binding domain that mediates binding to synectin (GIPC1) and in-turn regulates the endocytic trafficking of both NRP1 and VEGFR2 (Cai and Reed, 1999, Naccache et al., 2006, Horowitz and Seerapu, 2012, Lanahan et al., 2010). Accordingly, removal of the NRP1 cytoplasmic tail delays VEGFR2 endocytosis following VEGFA binding, leading to enhanced surface retention and reduced phosphorylation of tyrosine (Y)1175 in VEGFR2 (Lanahan et al., 2013). NRP1 thus acts as an important modulator of VEGFR2 activation and its downstream signalling pathways. However, reports have also suggested that VEGFA transduces biological responses in ECs via NRP1, in a VEGFR2-independent manner (Roth et al., 2016).

Global NRP1 knockout in mice results in lethality at E10-E12.5 due to abnormal vessel sprouting in major organs and impaired yolk sac vascularization (Kawasaki et al., 1999). Moreover, NRP1 overexpression leads to excessive vessel growth and promotes leaky and haemorrhagic vessels (Kitsukawa et al., 1995). Endothelial-specific knockout of NRP1 in mouse embryos only show mild embryonic brain defects, while in the adult vasculature no gross abnormalities are evident (Lanahan et al., 2013). Several reports also link increased NRP1 expression in tumours to a poor prognosis for survival (Miao et al., 2000, Kawakami et al., 2002, Hong et al., 2007). Furthermore, in diseases such as age related macular degeneration, NRP1 has been linked with increased neovascularization and vessel hyperpermeability, likely due to enhanced signalling downstream of VEGFA (Raimondi et al., 2014, Fernández-Robredo et al., 2017).

VEGFA-induced vascular permeability is mediated through the Y949 and Y1173 phosphosites of VEGFR2. The phosphorylated Y949 presents a binding site for TSAd (T-cell specific adaptor), which in turn binds SFKs (Src family kinases) that phosphorylate and promote internalization of junctional proteins such as VE-cadherin (Matsumoto et al., 2005, Sun et al., 2012, Li et al., 2016, Jin et al., 2022). Concurrently, pY1173 phosphorylates PLCY, leading to Ca2+/Protein kinase C (PKC) activation of endothelial nitric oxide synthase (eNOS), contributing to Src activation and phosphorylation of VE-cadherin (Sjoberg et al., 2023). The role of NRP1 in VEGFA-mediated permeability has been controversial. Studies employing *in* vivo and *in vitro* models have found NRP1 to be a positive regulator of VEGFA-mediated vascular permeability, or to lack effect, dependent on tissue or experimental setup (Fantin et al., 2017, Acevedo et al., 2008, Wang et al., 2015, Becker et al., 2005, Pan et al., 2007, Cerani et al., 2013). Additionally, treatment of ECs with CendR peptides, which bind and induce internalisation of NRP1, increases permeability in a NRP1-dependent, but VEGFR2-independent manner (Roth et al., 2016). Therefore, the exact role of NRP1 in VEGFA-VEGFR2 mediated permeability remains unclear. NRP1 is a promising target in a number of pathologies where vascular dysfunction is exacerbative. Understanding the relationship between NRP1 and VEGFA-VEGFR2 signalling is thus of potential therapeutic benefit.

Here, we aimed to further uncover the role of NRP1 in VEGFA-mediated vascular permeability. Using mice with global or EC-specific loss of NRP1 expression, we identify a tissue-specific role for endothelial NRP1 in the modulation of VEGFA/VEGFR2 signalling regulating vascular leakage. We find that endothelial-specific loss of NRP1 (*Nrp1* iECKO) can both increase and decrease VEGFA-mediated vascular leakage, dependent on the vascular bed. NRP1 is widely expressed and is an

important constituent of peri-vascular cells in some, but not all, tissues and vessel subtypes. The consequence of global loss of NRP1 expression demonstrates that peri-vascular NRP1 can modify VEGFA/VEGFR2-induced vascular leakage and steer the tissue-specific role of endothelial NRP1 in barrier integrity. Collectively, these data reveal that the relative expression levels of NRP1 between perivascular cells and ECs acts as a tissue-specific modifier of EC VEGFA/VEGFR2 signalling upstream of vascular leakage.

Results

NRP1 regulates VEGFA-mediated permeability in an organotypic manner

NRP1 has been studied extensively as a co-receptor of the VEGFA/VEGFR2 pathway, and its ability to modulate VEGFR2 signalling in developmental and pathological angiogenesis has been clearly established. However, results concerning the role of NRP1 in VEGFA-mediated vascular permeability have remained contradictory (Fantin et al., 2017, Acevedo et al., 2008, Wang et al., 2015, Becker et al., 2005, Pan et al., 2007, Cerani et al., 2013). $Nrp1^{fl/fl}$; $Cdh5^{CreERT2}$ (*Nrp1* iECKO) mice were used to study the EC-specific role of NRP1 in VEGFA-induced vascular leakage. Following tamoxifen administration, a 75% reduction in NRP1 protein levels was achieved in lung tissue, chosen for analysis due to the high EC content (**Figure 1A** and B). Furthermore, using immunofluorescent stainings, reduction in NRP1 levels could be observed in the ear and back skin vascular beds with the loss of EC NRP1 (**Supp. figure 1A** and B). Using a highly sensitive assay combining intravital microscopy and atraumatic intradermal microinjection in the ear skin of *Nrp1* iECKO mice, VEGFA-induced vascular leakage was significantly increased following the loss of NRP1 (**Figure 1C** and D) (Honkura et al., 2018). Additionally, we measured qualitative aspects of vascular leakage including lag period (time from stimulation to leakage onset) and degree of leakage (rate of dextran extravasation). These analyses showed that ECs in *Nrp1* iECKO mice respond faster to stimulation (**Figure 1E**) and exhibit more profuse leakage at each site (**Figure 1F**), indicative of increased disruption of EC-EC junctions. These data suggest that NRP1 exerts a stabilizing role by suppressing VEGFA-induced endothelial junction disruption in the ear dermis. This finding is in contrast to reports showing NRP1 to be a positive regulator of VEGFA-mediated vascular leakage (Fantin et al., 2017, Acevedo et al., 2008, Becker et al., 2005).

One possible explanation for these differences compared to previous reports is that the role of NRP1 may be organ dependent, in line with the growing insights into the distinct properties of ECs in different vessel types and vascular beds (Augustin and Koh, 2017). To investigate a potential organotypic role for NRP1 in EC biology, we studied the consequence of *Nrp1* knockout on the barrier properties of ECs in different vascular beds.

Initially, selected organs, chosen based on prior experience of their different EC barrier properties (Aird, 2007, Augustin and Koh, 2017, Richards et al., 2022), were investigated for their susceptibility to VEGFA-induced vascular leakage via the systemic administration of fluorescent dextrans with or without VEGFA. After 30 minutes, organs were collected and acute vascular leakage assessed microscopically or following solvent-based extraction of dextran and fluorescence spectroscopy. All organs analysed, except for the liver, showed vascular leakage after VEGFA stimulation (**Supp. figure 2A** - E). The role of endothelial NRP1 in these organs was further studied in *Nrp1* iECKO mice, showing significantly decreased VEGFA-mediated vascular leakage in the trachea and back skin (**Figure 1G** and H, **Supp. figure 3**). Kidney, skeletal muscle and heart in contrast did not show a significant difference in VEGFA-mediated vascular leakage following the loss of EC-expressed NRP1 (**Figure 1I** and J).

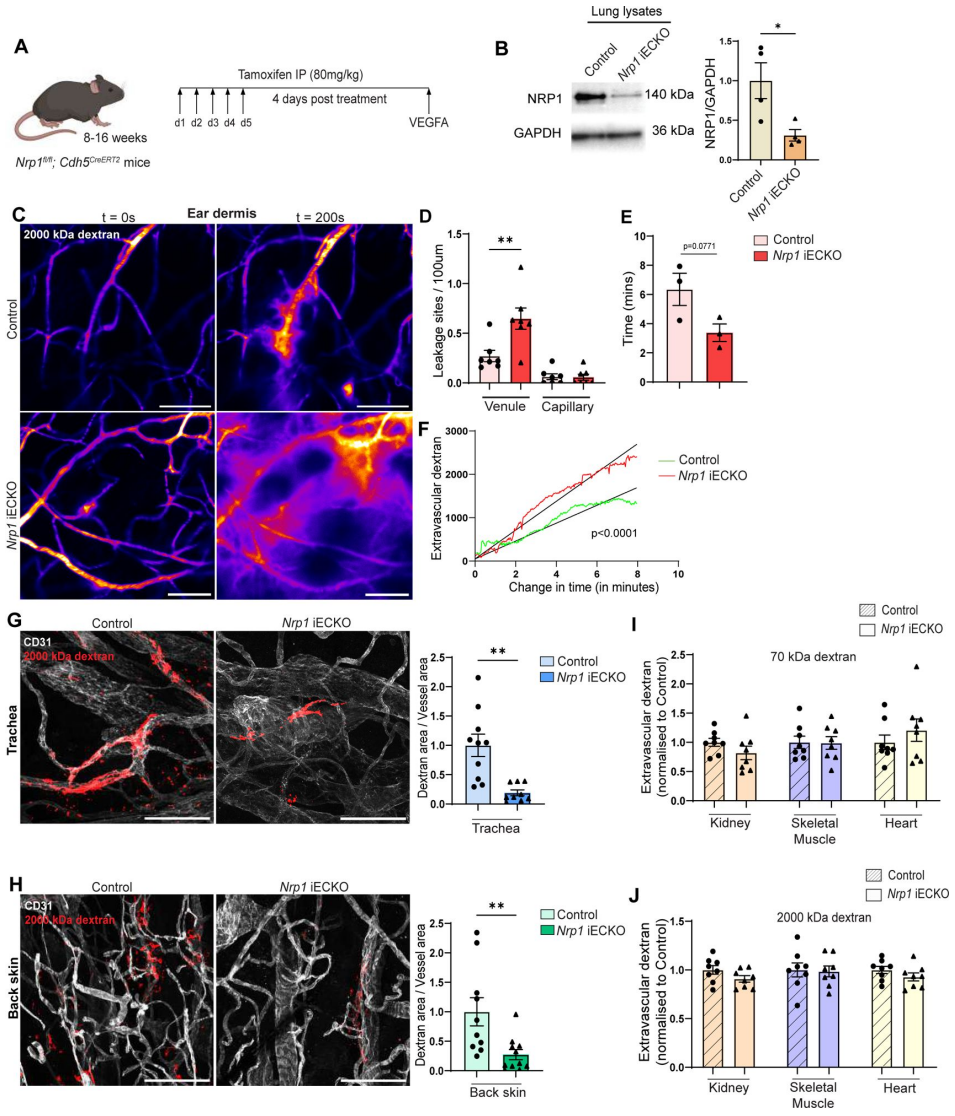

Figure 1

NRP1 regulates VEGFA-mediated permeability in an organotypic manner

(A) Schematic illustration of experimental design to induce recombination in *Nrp1* iECKO mice.
(B) Western blot quantification of lung lysates from tamoxifen-treated control and *Nrp1* iECKO mice (n=4).
(C) Representative images showing leakage of 2000 kDa FITC-dextran (Pseudo-colour) in response to intradermal VEGFA injection in the ear dermis of control and *Nrp1* iECKO mice.
(D) Leakage sites per vessel length in response to intradermal VEGFA stimulation in the ear skin of control and *Nrp1* iECKO mice. n=6 mice, two or more acquisitions/mouse.
(E) Lag period between intradermal VEGFA injection and initiation of leakage in the ear skin of control and *Nrp1* iECKO mice. n≥3 mice, two or more acquisitions/mouse, three or more sites/acquisition.
(F) Quantification of 2000 kDa dextran extravasation over time in the ear skin of control and *Nrp1* iECKO mice following intradermal VEGFA stimulation. Black lines represent lines of best fit for the slope between leakage initiation and leakage termination. n≥3 mice, two or more acquisitions/mouse, three or more sites/acquisition.
(G-H) Leakage of fixable 2000 kDa FITC dextran in trachea (G) and back skin (H) after systemic administration of VEGFA in control and *Nrp1* iECKO mice. Left, representative images. Right, quantification of tracer leakage area / vessel area (n ≥ 8 mice, 2 or more fields of view/mouse).
(I-J) Leakage of 70 kDa (I) and 2000 kDa (J) dextran extracted from perfused tissues after systemic administration of VEGFA in kidney, skeletal muscle and heart in control and *Nrp1* iECKO mice (n ≥ 8 mice).
Error bars; mean ± SEM. Statistical significance: Two-tailed unpaired student's t-test and linear regression with ANCOVA.
Scale bar: 100 μm

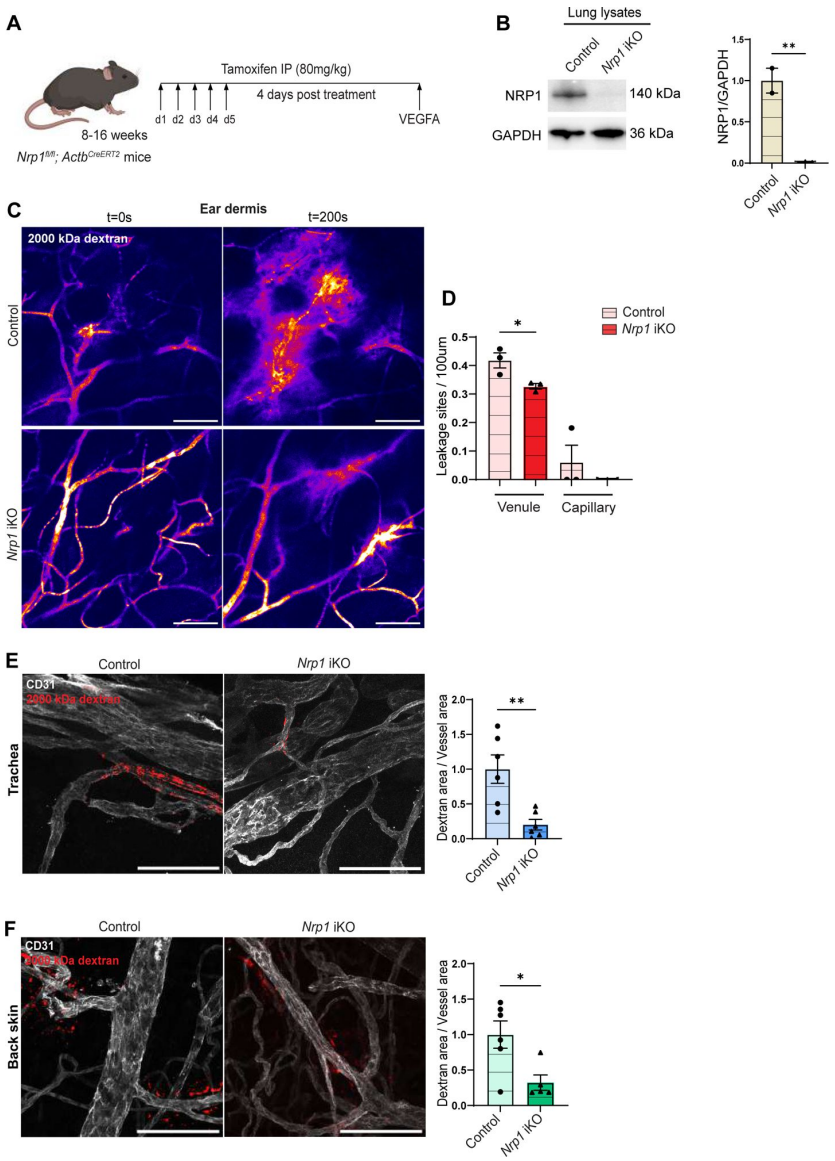

Figure 2

Global loss of NRP1 reduces VEGFA-mediated vascular permeability

(A) Schematic illustration of experimental design to induce recombination in *Nrp1* iKO mice.
(B) Western blot quantification of lung lysates from tamoxifen-treated control and *Nrp1* iKO mice (n ≥ 2 mice).
(C) Representative images showing leakage of 2000 kDa FITC dextran (Pseudo-colour) in response to intradermal VEGFA injection in the ear dermis of control and *Nrp1* iKO mice.
(D) Leakage sites per vessel length in response to intradermal VEGFA stimulation in the ear skin of control and *Nrp1* iKO mice. n=3 mice, two or more acquisitions/mouse.
(E-F) Leakage of fixable 2000 kDa FITC dextran in trachea (E) and back skin (F) after systemic administration of VEGFA in control and *Nrp1* iKO mice. Left, representative images. Right, quantification of tracer leakage area / vessel area (n ≥ 5 mice, 3 or more fields of view/mouse).
Error bars; mean ± SEM. Statistical significance: Two-tailed unpaired student's t-test. Scale bar: 100μm

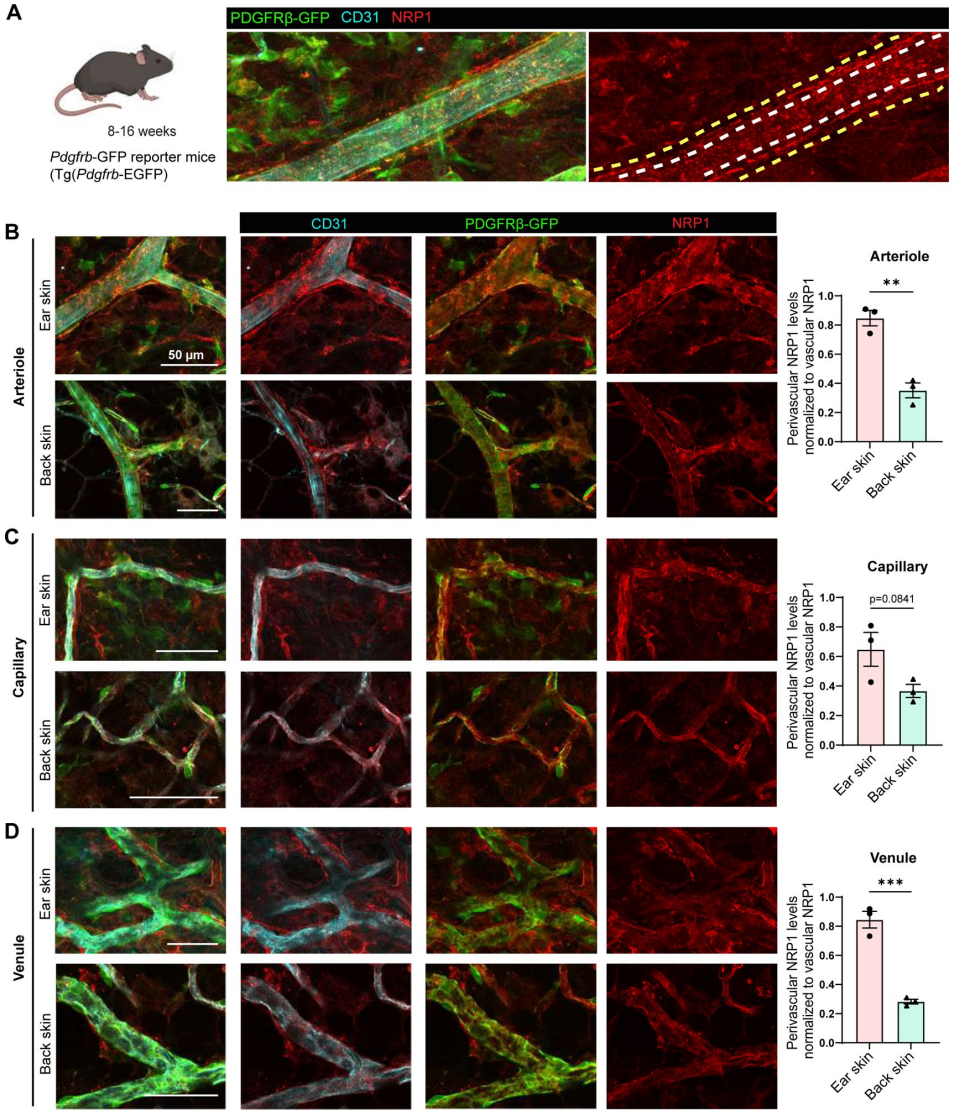

Figure 3

Heterogeneous expression of perivascular NRP1

(A) Schematic illusatration of mouse strain and representation of NRP1 expression in endothelial, and perivascular cells using *Pdgfrβ*-GFP mice. White dashed line encompasses vascular area, space between white and yellow dashed lines represents perivascular area. Note perivascular, NRP1 expressing cells in between yellow and white lines.
(B-D) Images, left, and quantification, right, showing vascular and perivascular NRP1 expression in arterioles **(A)**, capillaries **(B)** and venules **(C)** of ear skin and back skin and its relative expression.
Error bars; mean ± SEM. Statistical significance: Two-tailed unpaired student's t-test. Scale bar: 50µm

These data collectively suggest that endothelial NRP1 has an organ-specific role in controlling VEGFA-mediated vascular permeability. Importantly, endothelial NRP1 is a positive regulator of VEGFA mediated permeability in the trachea and back skin but a negative regulator in the ear skin.

Global inactivation of NRP1 reduces VEGFA-mediated vascular permeability

Our results here, where NRP1 may play positive (trachea and back skin), negative (ear skin) and passive (kidney, skeletal muscle and heart) role in VEGFA-induced vascular leakage, were collected using EC-specific knockout mice. In previous studies, mouse models of both EC-specific deletion and a globally expressed NRP1 C-terminal deletion mutant were employed (Fantin et al., 2017, Roth et al., 2016). We thus set out to investigate whether global inactivation of NRP1 using an anti-NRP1 blocking antibody might differently modify the VEGFA-induced leakage response. Wild-type C57Bl/6 mice were locally treated in the ear dermis with an anti-NRP1 antibody via intradermal injection, followed by intravital assessment of VEGFA-induced vascular permeability. Interestingly, NRP1 blockade reduced vascular leakage in the ear dermis when compared to isotype control (**Supp. figure 4A**). This is in contrast to the EC-specific loss of NRP1 in *Nrp1* iECKO mice, which resulted in enhanced VEGFA-mediated vascular leakage (**Figure 1C-F**). We similarly investigated the effect of blocking NRP1 on the back skin and tracheal vasculatures. Treatment with anti-NRP1 antibody was found to reduce VEGFA-induced leakage in both tissues following local and systemic administration of VEGFA respectively (**Supp. figure 4B** and C).

To verify the findings using neutralizing anti-NRP1 antibodies, we crossed $Nrp1^{fl/fl}$ with $Actb^{CreERT}$ mice to generate global *Nrp1* knock-out mice (*Nrp1* iKO). Efficient reduction of NRP1 protein was confirmed in lung lysates (**Figure 2A** and B). Complete loss of NRP1 could also be seen in the ear and back skin of these mice using immunofluorescent staining (**Supp. figure 1**). Intravital imaging of the ear dermis of *Nrp1* iKO mice showed that global loss of NRP1 reduced VEGFA-induced vascular leakage, in contrast to the phenotype seen in *Nrp1* iECKO mouse ear skin and in agreement with blocking antibody data (**Figure 2C** and D). Furthermore, global *Nrp1* knock-out resulted in a ~75% reduction in VEGFA-mediated vascular leakage also in the back skin and tracheal vasculatures, similar to that seen in *Nrp1* iECKO mice (**Figure 2E** and F).

These data illustrate the heterogenous nature of EC signalling regulation in different vascular beds, and show that NRP1 modulates VEGFA signaling in an organotypic and cell-specific manner. Notably, we demonstrate that VEGFA-induced leakage in the back skin and trachea is indistinguishable between endothelial-specific and global *Nrp1* KO mice, whereas in the ear skin there is a contrasting phenotype.

NRP1 is heterogeneously expressed in perivascular cells

NRP1 is known to form a heterocomplex with VEGFR2 upon VEGFA binding. Interestingly, VEGFR2/NRP1/VEGFA can assemble as a juxtacrine *trans* complex, where NRP1 and VEGFR2 are expressed on the surface of adjacent cells, as well as a *cis* complex, where NRP1 and VEGFR2 are expressed on the same cell (Koch et al., 2014). Importantly, even though the kinetics of *trans* VEGFR2/NRP1 complex formation is slow, these complexes are stable and produce a distinct signalling output compared to the *cis* configuration (Koch et al., 2014). Thus, NRP1 presented in *cis* or *trans* produces differential VEGFR2 signalling output upon VEGFA binding. Given the above findings we reasoned that peri-endothelial distribution of NRP1 could be an important modifier of EC VEGFR2 signalling and possibly explain organotypic differences observed in *Nrp1* iECKO mice.

To investigate the pattern of NRP1 expression we employed a *Pdgfrβ* promoter-driven GFP (*Pdgfrβ-GFP*) mouse to visualize PDGFRβ-positive pericytes. To visualize ECs, and the localization of NRP1 in the ear skin and back skin from these mice, tissues were immunostained for CD31 and NRP1, respectively. NRP1 expression could be seen in both endothelial and perivascular cells, which was

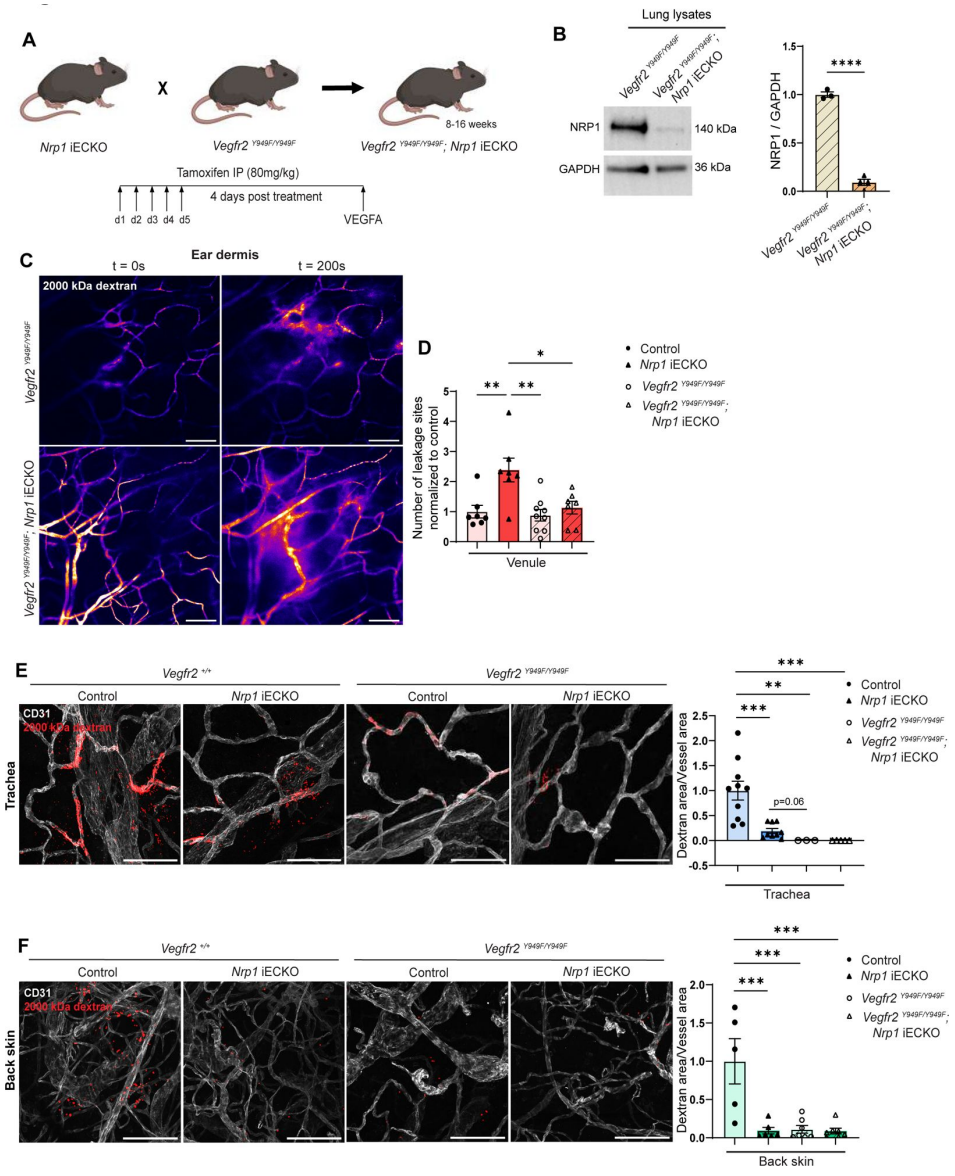

Figure 4

NRP1 distribution modifies VEGFA-induced vascular permeability

(A) Schematic illustration of breeding scheme to obtain homozygous *Vegfr2* $^{Y949F/Y949F}$; *Nrp1* iECKO mice and experimental design to induce recombination.
(B) Western blot quantification of lung lysates from tamoxifen treated *Vegfr2* $^{Y949F/Y949F}$ and *Vegfr2*$^{Y949F/Y949F}$; *Nrp1* iECKO mice (n=3 mice).
(C) Representative images showing leakage in response to intradermal VEGFA injection in the ear dermis of *Vegfr2* $^{Y949F/Y949F}$ and *Vegfr2* $^{Y949F/Y949F}$; *Nrp1* iECKO mice.
(D) Leakage sites per vessel length in response to intradermal VEGFA stimulation in the ear skin of in control, *Nrp1* iECKO, *Vegfr2* $^{Y949F/Y949F}$ and *Vegfr2* $^{Y949F/Y949F}$; *Nrp1* iECKO mice, normalized to control (n ≥ 6 mice, two or more acquisitions/mouse).
(E-F) Leakage of 2000 kDa dextran in trachea (E) and back skin (F) of control, *Nrp1* iECKO, *Vegfr2* $^{Y949F/Y949F}$and *Vegfr2* $^{Y949F/Y949F}$; *Nrp1* iECKO mice after systemic administration of VEGFA. Left, representative images. Right, quantification of tracer leakage area/vessel area (n ≥ 3 mice, 2 or more fields of view/mouse).
Error bars; mean ± SEM. Statistical significance: Two tailed unpaired student's t-test and Two-way ANOVA. Scale bar: 100µm

lost after global *Nrp1* deletion (**Figure 3A** and **Supp. Figure 1**). Both arteriolar (**Figure 3B**) and capillary (**Figure 3C**) PDGFRβ-positive perivascular cells expressed NRP1. The relative level of perivascular/EC expression of NRP1 was higher in the ear skin compared to back skin. In venules, the low expression of NRP1 in perivascular cells in the back skin resulted in a 5-fold difference in the perivascular/EC NRP1 ratio, when comparing the ear skin to back skin (**Figure 3D**).

These data thus show that NRP1 is expressed in perivascular cells of the ear skin and back skin. We find however that the ratio of NRP1 expression between ECs and perivascular cells differs between ear skin and back skin, and between different vessel types. In ear skin the perivascular/EC ratio is higher compared to the back skin, which may support a higher ratio of *trans* NRP1/VEGFR2 relative to cis complexes in the ear skin.

NRP1 distribution modifies VEGFA-mediated signalling and vascular leakage

NRP1 modifies VEGFR2 signalling by controlling its internalisation and intracellular trafficking (Bayliss et al., 2020, Ballmer-Hofer et al., 2011). The presence of NRP1 in *trans* however, modifies this dynamic and retains VEGFR2 at the cell surface for longer time periods, altering its signalling output (Koch et al., 2014).

We thus wished to investigate whether perivascular NRP1 expression might interact with and alter VEGFR2 signalling upstream of vascular leakage, and explain the above described organotypic effects of EC NRP1 loss. For this purpose, *Nrp1* iECKO mice were crossed with homozygous $Vegfr2^{Y949F/Y949F}$mice, to produce $Vegfr2^{Y949F/Y949F}$;*Nrp1* iECKO mice that are deficient in both EC NRP1 expression and VEGFA-mediated vascular leakage ability. In these mice, loss of NRP1 protein was efficiently established in lung tissue (**Figure 4A** and B). Analysis of VEGFA-mediated vascular leakage in the ear dermis showed that the increased leakage, induced by the loss of EC NRP1, was abrogated by the loss of the VEGFR2 phosphosite Y949, known to be required for activation of Src in response to VEGFA (**Figure 4C** and D). These analyses suggest that, in the ear dermis, EC NRP1 negatively regulates VEGFA-induced vascular leakage by modulation of VEGFR2 activation and phosphorylation.

We next sought to determine the relationship between NRP1 and VEGFR2 Y949 signalling in the trachea and back skin vasculatures. Leakage in $Vegfr2^{Y949F/Y949F}$;*Nrp1* iECKO mice was induced by systemic VEGFA and fluorescent 2000 kDa dextran administration in both *Nrp1* iECKO and $Vegfr2^{Y949F/Y949F}$;*Nrp1* iECKO mice. As we observed previously, loss of EC NRP1 reduced vascular leakage in the trachea and back skin by 75%, an effect that was enhanced further by the VEGFR2 Y949F mutation (**Figure 4E** and F). Importantly, leakage was similarly inhibited in the $Vegfr2^{Y949F/Y949F}$ model as in the combined $Vegfr2^{Y949F/Y949F}$;*Nrp1* iECKO mice in both the trachea and back skin. These data show that NRP1 presented in *trans* by perivascular cells in the ear dermis can signal through VEGFR2 to induce vascular leakage, and that VEGFR2 Y949 is vital for mediating NRP1's effects on endothelial junctions.

Perivascular NRP1 modifies VEGFA-induced signalling

VEGFA/VEGFR2 signalling mediates phosphorylation of VE-Cadherin on Y685, required for vascular permeability (Orsenigo et al., 2012, Wessel et al., 2014). We have also recently shown that PLCγ is an important mediator of VEGFA-induced vascular leakage by allowing the production of nitric oxide through eNOS, which in turn modified Src by tyrosine nitration, required for full Src activity (Sjoberg et al., 2023). To clarify the impact of perivascular NRP1 on VEGFA-induced signalling we studied VE-Cadherin and PLCγ phosphorylation in *Nrp1* iECKO and *Nrp1* iKO mice (**Figure 5**). Perivascular NRP1 expression in the ear dermis of *Nrp1* iECKO mice was lost in *Nrp1* iKO mice (**Supp. figure 1**). In agreement with the enhanced vascular leakage in the ear dermis of *Nrp1* iECKO mice, VE-Cadherin phosphorylation at Y685 was enhanced following intradermal

VEGFA injection (**Figure 5A**). No such induction was seen in *Nrp1* iKO mice (**Figure 5B**). In the back skin, VE-Cadherin pY685 levels were induced by VEGFA in the control but not in the *Nrp1* iECKO, nor the iKO models (**Figure 5C** and D), in accordance with the permeability phenotype (see **Figure 1**). Similarly, PLCγ phosphorylation was potentiated in the ear skin of *Nrp1* iECKO but not *Nrp1* iKO mice (**Supp. figure 5A** and B). Moreover, in the back skin loss of either endothelial or global NRP1 led to a reduction in PLCγ phosphorylation following intradermal VEGFA stimulation (**Supp. figure 5C** and D).

Taken together these data show that NRP1 is expressed by perivascular cells in a tissue-specific manner and that perivascular NRP1 can be an important modulator of VEGFA-signalling. In the ear dermis, NRP1 is expressed by both endothelial and perivascular cells, forming *cis* and *trans* interactions with VEGFR2 respectively. Whilst the *cis* EC interaction predominates, loss of EC NRP1 promotes *trans* NRP1/VEGFR2 interaction and potentiates VEGFA-induced signalling regulating vascular leakage (**Figure 6**). Meanwhile, due to a paucity of perivascular NRP1 in the trachea and back skin vasculatures, loss of EC NRP1 leads to a loss of NRP1:VEGFR2 complexes, attenuating VEGFA-regulated vascular leakage.

Discussion

Here we find that NRP1 expression by perivascular cells is an important modulator of VEGFA signalling regulating endothelial junction stability. Our data suggest that NRP1 presented in a juxtacrine manner can potentiate certain VEGFR2 signalling upstream of vascular leakage. NRP1 is expressed by a number of cells adjacent to blood vessels, including PDGFRβ-positive pericytes. However, the abundance of these cells and their level of NRP1 expression differ between vascular beds. Loss of EC-specific NRP1 thus has a differential effect on VEGFA-mediated vascular leakage in different vascular beds, dependent on the ability of ECs to form *trans* NRP1/VEGFR2 complexes.

Numerous studies have implicated endothelial NRP1 as a positive regulator of permeability (Fantin et al., 2017, Becker et al., 2005, Acevedo et al., 2008). However, multiple studies argue against this, with NRP1 blockade or deletion having no effect on VEGFA-induced vascular leakage in the skin and retina (Pan et al., 2007, Cerani et al., 2013). Here we find that the function of endothelial NRP1 in VEGFA-mediated vascular permeability varies in different vascular beds. In keeping with previous data, we find that loss of NRP1 reduces VEGFA-induced vascular leakage in the back skin and trachea. Meanwhile, endothelial NRP1 appears to have no effect on VEGFA-induced vascular leakage in kidney, skeletal muscle and heart. In the ear skin, however, loss of NRP1 surprisingly leads to an increase in VEGFA-induced vascular leakage. This appears to be through enhanced VEGFR2 Y949 signalling, as mutation of this phosphosite normalises the enhanced leakage seen after loss of NRP1. Previous publications have described NRP1 as being pivotal for VEGFR2-induced Src activity via recruitment of Abl kinase (Fantin et al., 2017). How exactly VEGFA-VEGFR2 signals to Abl, and whether this requires the Y949 phosphosite, however is unknown. Further work is required to understand exactly how NRP1 modifies VEGFR2 activity and how this differs between different vascular beds.

As others have noted and we see here, NRP1 is expressed by perivascular cells, including PDGFRβ positive pericytes (Bartlett et al., 2017, Wnuk et al., 2017). However, we find that perivascular NRP1 expression and its ratio to EC expression differs between different vascular beds, being higher in the ear skin than back skin. When the *trans* NRP1/VEGFR2 complex predominates, as in the ear skin of *Nrp1* iECKO mice, our data indicate that VEGFA/VEGFR2 signalling impacting junction stability is potentiated. This is in keeping with reports showing that NRP1 presented in *trans* can modify VEGFR2 signalling kinetics, resulting in prolonged PLCγ and ERK2 phosphorylation (Koch et al., 2014). However how such prolonged kinetics might affect the VEGFR2 signalling pathways upstream of vascular leakage has not been previously explored. In addition, juxtacrine NRP1 interactions have been shown to have important functions in cell types

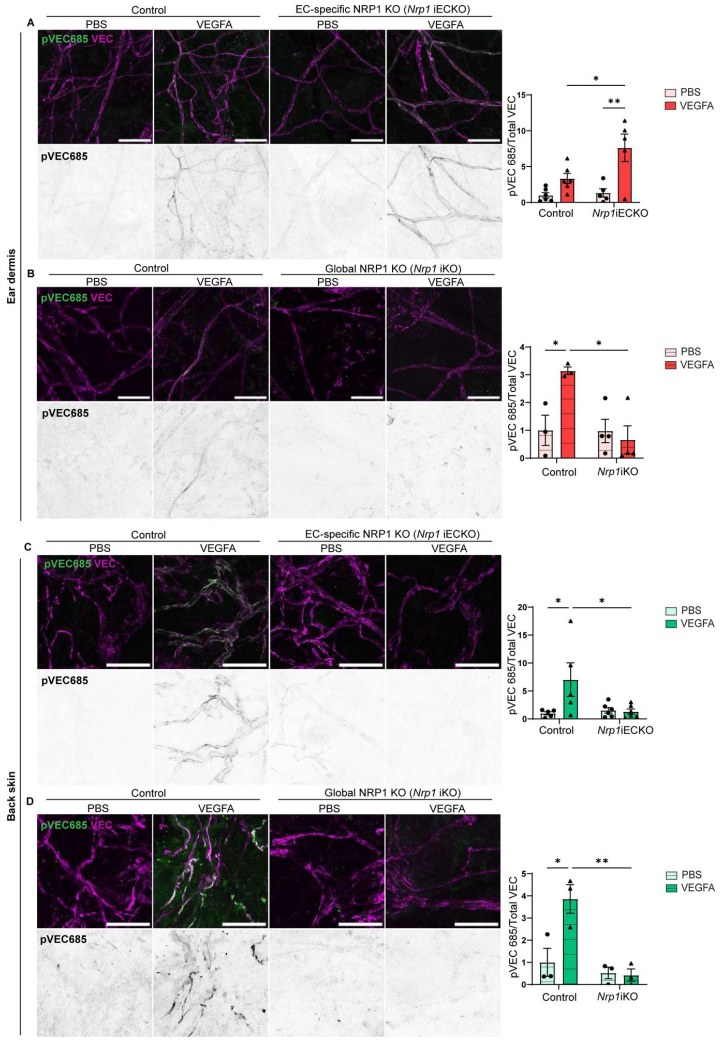

Figure 5

Perivascular NRP1 modifies VEGFA-induced signalling

(A-B) Phosphorylation of VE-Cadherin (VEC) Y685 in response to intradermal PBS or VEGFA injections in the ear dermis of control and *Nrp1* iECKO (A) or *Nrp1* iKO (B) mice. Left, representative images.
Right, quantification of phosphorylated VEC Y685 area per total VEC area normalized to PBS control in the ear dermis of control and *Nrp1* iECKO or *Nrp1* iKO mice. n≥3 mice, two or more fields of view/mouse.
(C-D) Phosphorylation of VE-Cadherin Y685 in response to intradermal PBS or VEGFA injections in the back skin of control and *Nrp1* iECKO (C) or *Nrp1* iKO (D) mice. Left, representative images. Right, quantification of phosphorylated VEC Y685 area per total VEC area normalized to PBS control in the back skin of control and *Nrp1* iECKO or *Nrp1* iKO mice. n≥3 mice, two or more fields of view/mouse.
Error bars; mean ± SEM. Statistical significance: Two-way ANOVA. Scale bar: 50μm

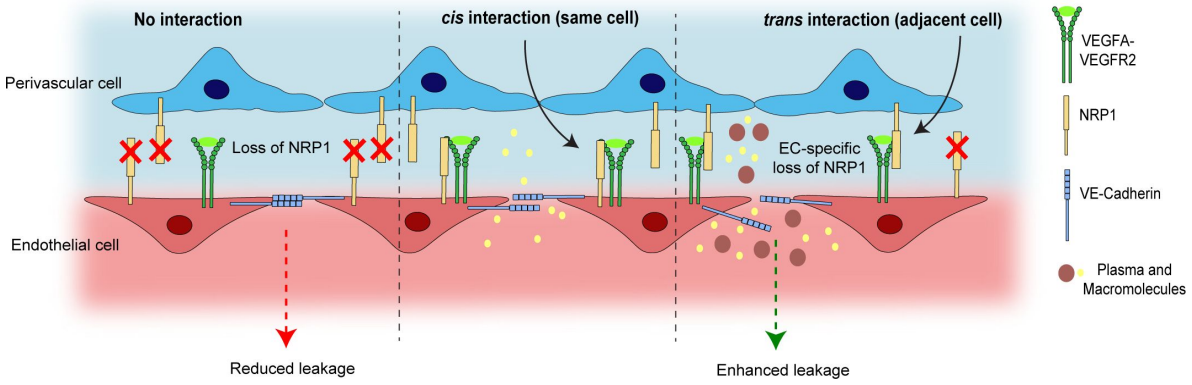

Figure 6

Schematic model of NRP1's spatial effects on VEGFA-induced vascular permeability

With global loss of NRP1, VEGFA/VEGFR2 signalling regulating vascular leakage is suppressed and thus leakage is reduced (left). In the presence of EC NRP1, a VEGFA/VEGFR2/NRP1 complex is formed in *cis,* which has a rapid and transient effect on VEGFR2 downstream signalling (middle). Loss of EC NRP1 but the presence of perivascular NRP1 leads to formation of a stable VEGFA/VEGFR2/NRP1 complex in *trans* and enhanced VEGFR2 signalling and increased vascular permeability.

other than ECs. For example, NRP1 expressed on microglia is important for the trans-activation of PDGFRα on oligodendrocyte precursor cells, resulting in enhanced proliferation and myelin repair (Sherafat et al., 2021). Furthermore, NRP1 has been posited as a potential immune checkpoint inhibitor (Sarris et al., 2008). NRP1 is highly expressed by regulatory T cells, as well as antigen presenting dendritic cells, and the formation of *tran*s NRP1 homodimers has been suggested to stabilise regulatory T cell function and promote immune tolerance. Finally, numerous studies have described the expression of NRP1 on tumour cells, which can modify EC behaviour and alter their angiogenic potential (Koch et al., 2014, Miao et al., 2000, Hu et al., 2007, Shahrabi-Farahani et al., 2016). This may partly be due to the ability of NRP1 to bind VEGFA and thus provide a pool of tumoural VEGFA towards which ECs migrate. In tumours, NRP1 can also form juxtacrine interactions with VEGFR2 on ECs upon VEFGA binding and modify intracellular EC signalling compared to NRP1 action in a *cis* manner (Koch et al., 2014, Morin et al., 2020, Morin et al., 2018).

One possible mechanism by which NRP1 presented in *trans* might alter VEGFA/VEGFR2 signalling, when compared to *cis*, is via modification of VEGFR2 trafficking. The adapter molecule synectin is an important intracellular binding partner of NRP1 and facilitates myosin IV-mediated endocytosis (Cai and Reed, 1999, Naccache et al., 2006). A recent study also found that NRP1 interacts with members of the ERM family of intracellular proteins, which act as intermediaries between the plasma membrane and actin cytoskeleton and that have also been associated with endocytosis and intracellular trafficking (Ponuwei, 2016, Gioelli et al., 2022). NRP1 may thus function not just as a co-receptor, but also as a linker to mediate the intracellular trafficking of cell surface receptors. This idea is supported by studies showing that NRP1 co-ordinates PDGFRα internalisation and its intracellular signalling, as well as the trafficking of integrin α5β1 during cell adhesion (McGowan and McCoy, 2021). Furthermore, it has recently been shown that NRP1 binds to VE-Cadherin and regulates its cell surface turnover, a role that has been proposed to at least partly explain its role in EC barrier integrity (Gioelli et al., 2022, Bosseboeuf et al., 2023). In response to VEGFA the cytoplasmic domain of NRP1, which binds synectin, has been found to be crucial in mediating NRP1's positive regulation of leakage (Fantin et al., 2017). Furthermore, mutant mice lacking the NRP1 cytoplasmic domain have impaired arteriogenesis due to delayed VEGFR2 endocytosis and resulting reduction in phosphorylation at Y1175 (Lanahan et al., 2013). Interestingly, the C-terminal tail is also crucial for the stability of trans NRP1-VEGFR2 complexes (Koch et al., 2014). A central function of NRP1 is thus to mediate VEGFR2 internalisation and trafficking following VEGFA stimulation. From our data we hypothesise that NRP1 presented in *trans* delays VEGFR2 internalisation and potentiates VEGFR2 signalling upstream of vascular leakage. Indeed, a recent study found that proper internalisation of VEGFR2 is required to shutdown VEGFR2 Y949 signalling through increasing the stoichiometric ratio of cell surface phosphatases that dephosphorylate Y949 (Corti et al., 2022). Our data are compatible with the hypothesis that VEGFR2 held at the cell surface via juxtracrine NRP1 interaction is capable of enhancing VEGFR2 Y949 signalling and resulting disruption of EC junctions, but due to the rapid turnover of VEGFR2 phosphorylation, this is technically very challenging to conclusively demonstrate. We hypothesize however that NRP1 expression within the perivascular microenvironment could be an important modifying factor of EC signalling and function, and might play an important role in mural cell function during vascular development and quiescence.

Combined, we identify a differential function of endothelial NRP1 in VEGFA-mediated vascular leakage in different vascular beds. Different levels and patterning of perivascular NRP1 expression has the potential to modify VEGFR2 signalling and alter VEGFA-induced vascular hyperpermeability. Further elucidation of NRP1 expression patterns in different tissues and how the VEGFA/NRP1/VEGFR2 complex presented in *cis* or *trans* can differentially modify cellular signalling will allow to better understand how NRP1 may serve in therapeutic applications in a distinct manner in different tissues.

Acknowledgements

We thank the BioVis imaging facility, Uppsala University, for expert services. We appreciate expert advice from Dr. Konstantin Gängel. This study was supported by the Swedish Research Council (2022-00896), the Knut and Alice Wallenberg foundation (KAW 2020.0057 and KAW 2019.0276), Fondation Leducq Transatlantic Network of Excellence Grant in Neurovascular Disease (17 CVD 03) to LCW. MR was supported by Olle Engkvist (218-0057) SSMF (201912) and an EMBO long-term fellowship (ALTF 923–2016).

Author contributions

Conceptualization, M.R. and L.C.-W.; methodology, M.R. and S.P.; investigation, M.R., S.P., Y.S.; writing, M.R., S.P. and L.C.-W.; funding acquisition; M.R. and L.C.-W.; resources, L.C.-W.

Conflict of interest

M.R. is now an employee for AstraZeneca (Biopharmaceuticals R&D, Cambridge, UK). All of this work was performed at Dept. of Immunology, Genetics and Pathology, Beijer and Science for Life Laboratories, Uppsala University, Uppsala, Sweden. No funding or support was received from AstraZeneca. Other authors declared no conflict of interest.

Methods

Animals

In vivo animal experiments were carried out in accordance with the ethical permit provided by the Committee on the Ethics of Animal Experiments of the University of Uppsala (permit 6789/18). *Nrp1*$^{flox/flox}$ mice contain *loxP* sites flanking exon 2 and were obtained from The Jackson Laboratory (005247). This strain was crossed with Cdh5(PAC)-CreER^{T2} mice (kind gift from Dr. Ralf Adams, Max-Planck Institute Münster) or Tmem163Tg(ACTB-cre)2Mrt mice to generate endothelial-specific *Nrp1* iECKO mice and global *Nrp1* iKO mice respectively. Mice possessing a knock-in mutation in the VEGFR gene, *Kdr*, at the Y949 phosphosite have been described previously (Li et al., 2016). These mice were crossed with *Nrp1* iECKO mice to generate *Vegfr2* $^{Y949F/Y949F}$*; Nrp1* iECKO mice. *Pdgfrb*-GFP reporter mice (Tg(Pdgfrb-EGFP)jn169Gsat/Mmucd, Stock number 031796-UCD) have been described previously (Jung et al., 2018). Mice were maintained in ventilated cages with group housing (2–5 per cage) and access to water and feed ad libitum. Male and female mice age 8-18 weeks were used. Each experiment was conducted on tissue from at least three age-matched animals representing individual biological repeats. Sample size (number of acquired images / movies and number of mice) were chosen to ensure reproducibility and allow stringent statistical analysis. To induce Cre recombinase-mediated gene recombination tamoxifen (SigmaAldrich, T5648) formulated in peanut oil was injected intraperitoneally (80 mg/kg) for 5 consecutive days. The mice were allowed to rest for 4 days before experiments were conducted.

Intravital vascular leakage assay

Intravital imaging of the mouse ear with intradermal injection has been described previously (Honkura et al., 2018). Briefly, following systemic administration of 2000 kDa FITC (SigmaAldrich, FD2000S) or TRITC Dextran (ThermoFischer Scientific, D7139) by tail-vein injection, mice were sedated by intraperitoneal injection of Ketamine-Xylazine (120 mg/kg Ketamine, 10 mg/kg Xylazine) and the ear secured to a solid support. Mice were maintained at a body temperature of 37 °C for the entire experiment, maximum 90 min. Time-lapse imaging was performed using single-photon microscopy (Leica SP8). For intradermal EC stimulation, a volume of approximately 0.1 µl VEGFA (Peprotech, 450-32), concentration 100 ng/µl, was injected using a sub-micrometer capillary needle. 10 kDa TRITC Dextran (ThermoFischer Scientific, D1817) was used as a tracer. Leakage sites were identified in time-lapse imaging as defined sites of concentrated dextran in the extravascular space.

Miles' assay

Mice were injected intraperitoneally with pyrilamine maleate salt (4mg/kg, Sigma, P5514) diluted in 0.9% saline, to inhibit histamine release, 30 min prior to tail vein injection of Evans blue (100 µl, 1% Evans blue). Evans blue was allowed to circulate for 10 min before intradermal injection in the back skin of recombinant mouse VEGFA165 (Peprotech, 450-32) (80 ng in 25 µl) or PBS. The skin was excised 30 minutes subsequent to VEGFA injection, placed in formamide over night at 55°C and absorbance at 620nm was measured using a spectrophotometer and normalized to tissue weight.

Systemic VEGFA-induced permeability

To assess EC permeability, all tissues were cleaned of excess cartilage, fat and connective tissue. Skeletal muscle was assessed using the tibialis anterior and liver was assessed using the left lateral lobe. To analyse liver, kidney, skeletal muscle and heart permeability, dextran (30 mg/kg) with or without VEGFA (160 µg/kg) were injected systemically through the tail vein. Thirty minutes later mice were anesthetized with Ketamine/Xylazine before intracardiac perfusion with Dulbecco's phosphate buffered saline (DPBS). Tissues were dissected, washed in DPBS and incubated in formamide for 48 hr at 55 °C. Dextran fluorescence was then measured using a spectrophotometer and normalized to tissue weight. To assess VEGFA-induced leakage microscopically, mixtures of fixable dextran (FITC, Tdb labs; TRITC, ThermoFischer Scientific, D7139) (30 mg/kg) with VEGFA (160 µg/kg) were injected systemically through the tail vein. Thirty minutes later mice were anesthetized with Ketamine/Xylazine before intracardiac perfusion with DPBS followed by 1% paraformaldehyde. Tissues were then immersed in 1% paraformaldehyde for 2 hr before proceeding with immunohistochemistry. For leakage quantification at least three large tile scan areas (≥1 mm^2) were captured for each mouse.

Intradermal VEGFA injection in the ear and back skin

Mice were anesthetised using isofluorane and injected with PBS or VEGFA (Peprotech, 450-32) (20ug in 5 ul for the ear dermis and 80ug in 20ul for the back skin) followed by perfusion using 1% PFA. The ear and back skin samples were excised and further fixed for 1 hour in 1% PFA. Afterwards, the tissue samples were processed for immunostaining.

NRP1 blockade

Anti-NRP1 (R&D systems, MAB59941) or isotype control (R&D Systems, MAB006) were administered intradermally in the ear skin (1 µg) or back skin (5 µg), or systemically (2 mg/kg). 24 hours later VEGFA-mediated vascular leakage was assessed using the intravital vascular leakage assay, Miles' assay or through systemic VEGFA-induced permeability.

Immunohistochemistry

Tissues were fixed through intracardiac perfusion with 1% paraformaldehyde (PFA) followed by immersion in 1% PFA for 2 hr at room temperature. For whole mount preparation of the ear skin, back skin and trachea removal of excess cartilage, fat and connective tissue tissues was carried out. Tissues were blocked overnight at 4 °C in Tris-buffered saline (TBS), 5% (w/v) Bovine Serum Albumin (BSA), 0.2% Triton X-100. Samples were incubated overnight with primary antibody in blocking solution, followed by washing in TBS, 0.2% Triton X-100 and incubation with appropriate secondary antibody for 2 hr at room temperature in blocking buffer before washing and mounting in fluorescent mounting medium (DAKO). Images were acquired using a Leica SP8 confocal microscope. Commercial antibodies used were: rat anti-CD31 (BD Biosciences, 553370), goat anti-CD31 (R&D Systems, AF3628), goat anti-NRP1 (R&D Systems, AF566), chicken anti-GFP (Abcam, Ab13970), rabbit anti-phospho-PLCγ1 (Tyr783) (Cell signaling technology, 2821s), rabbit anti-PLCγ1 (Cell signaling technology, 2822s), and goat anti–VE-cadherin (R&D systems, AF1002). Secondary antibodies against rat (ThermoFischer Scientific; Alexa 488, A21208 and Alexa 594, A21209), rabbit (ThermoFischer Scientific; Alexa 488, A21206 and Alexa 568, A10042), goat (ImmunoResearch Laboratories, Alexa 647, 705-605-147), chicken (ImmunoResearch Laboratories, Alexa 488, 703-545-155) were used. pVEC Y685 antibody was prepared by immunizing rabbits with phospho-peptides of the corresponding region in mouse VE-cadherin (New England Peptide) and further verified using immunostaining in $Cdh5^{Y685F/Y685F}$ mice. Primary and secondary antibodies were prepared at a dilution of 1:100 and 1:400, respectively unless otherwise stated.

Western blot analysis

Lungs from mice were removed and snap frozen. Protein was obtained by mechanical dissociation in RIPA buffer supplemented with 50 nM Na3VO4, Phosphatase inhibitor cocktail (Roche 04906837001) and Protease inhibitor cocktail (Roche, 04693116001). LDS sample buffer (Invitrogen, NP0007) and Sample Reducing Agent (Invitrogen, NP0009) were added to the samples and heated to 70 °C for 10 min. Proteins were separated on Nu Page 4–12% Bis-Tris Gel (Invitrogen) in MOPS SDS Running buffer (Invitrogen, NP0001), transferred to PVDF membrane (Thermo scientific, 88518) in NuPAGE transfer buffer (Novex, NP006), 10% methanol and subsequently blocked with 5% BSA in Tris-buffered saline with Tween 20 (TBST) for 60 min. The immunoblots were analysed using primary antibodies incubated overnight at 4 °C and secondary antibodies linked to horseradish peroxidase (HRP) (Cytiva) incubated for 1 hr at room temperature. After each step filters were washed four times with TBST. HRP signals were visualized by enhanced chemiluminescence (ECL) (Cytiva) (1:25000) and imaged with Chemidoc (Bio-Rad).

Primary antibodies targeting GAPDH (Chemicon, MONOCLONAL ANTIBODY374), NRP1 (R&D Systems, AF566) were used at a dilution of 1:1,000.

Image quantification

For confocal images, macromolecular leakage was quantified by measurement of tracer area following image thresholding. Tracer area was then normalized to vessel area. For analysis of vascular and peri-vascular NRP1 expression, masks were generated of the CD31 vascular area and the peri-vascular area 3μm around the vessel (**Figure 3A**). NRP1 area following thresholding was quantified within, and normalised to these areas. Phosphorylation values were quantified by measurement of phosphorylated vessel area following image thresholding. Phosphorylation area was then normalized to vessel area. Threshold values were kept constant within experiments.

Analysis of leakage from intravital movies has been described previously (Richards et al., 2021). Briefly, leakage sites were identified in time-lapse imaging as defined sites of concentrated dextran in the extravascular space. To quantify these their numbers were normalized to vessel length. To

assess lag period the time of the appearance of these sites following injection of stimulus was quantified. To assess the extent of barrier disruption the rate of dextran extravasation specifically at these sites was quantified over time.

All measurements were done with Fiji processing package of Image J2 software.

Statistical analysis

Data are expressed as mean ± SEM. The statistical tests used were the Students't test and two-way ANOVA. P-values given are from independent samples analysed by two-tailed paired t tests or multiple comparisons obtained from two-way ANOVA. Rate of leakage was compared using linear regression and ANCOVA. All statistical analyses were conducted using GraphPad Prism. A p-value <0.05 was considered statistically significant and significances indicated as $p<0.05$ (*), $p<0.01$ (**), and $p<0.001$ (***). For animal experiments, no statistical methods were used to predetermine sample size. The investigators were blinded to allocation during experiment and outcome assessment.

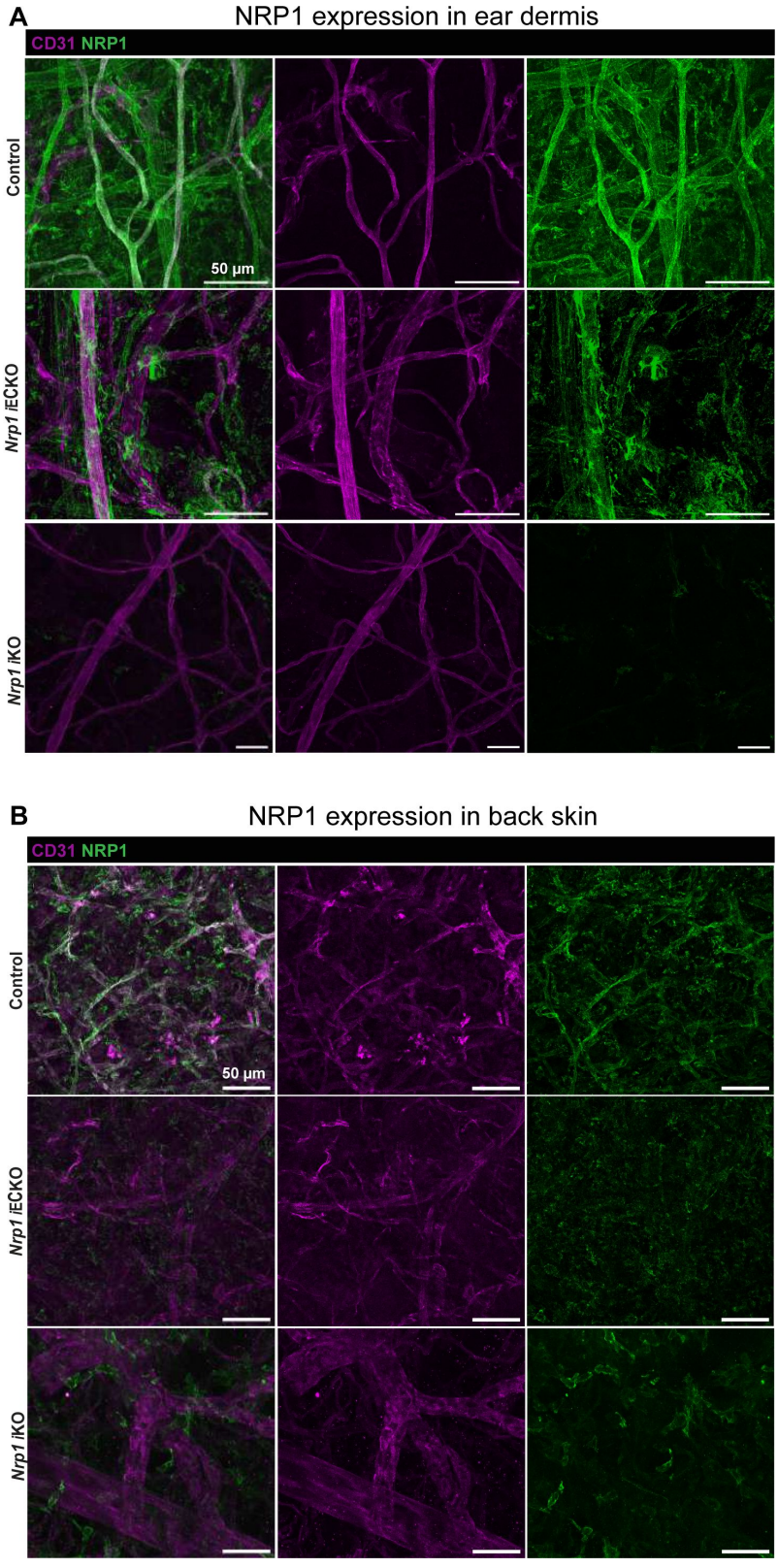

Supplementary Figure 1.

NRP1 expression in the ear dermis and back skin of adult mice

(A-B) Whole mount immunostainings showing NRP1 expression in ear dermis (A) and back skin (B) of control, *Nrp1* iECKO and *Nrp1* iKO mice. Scale bar: 50µm

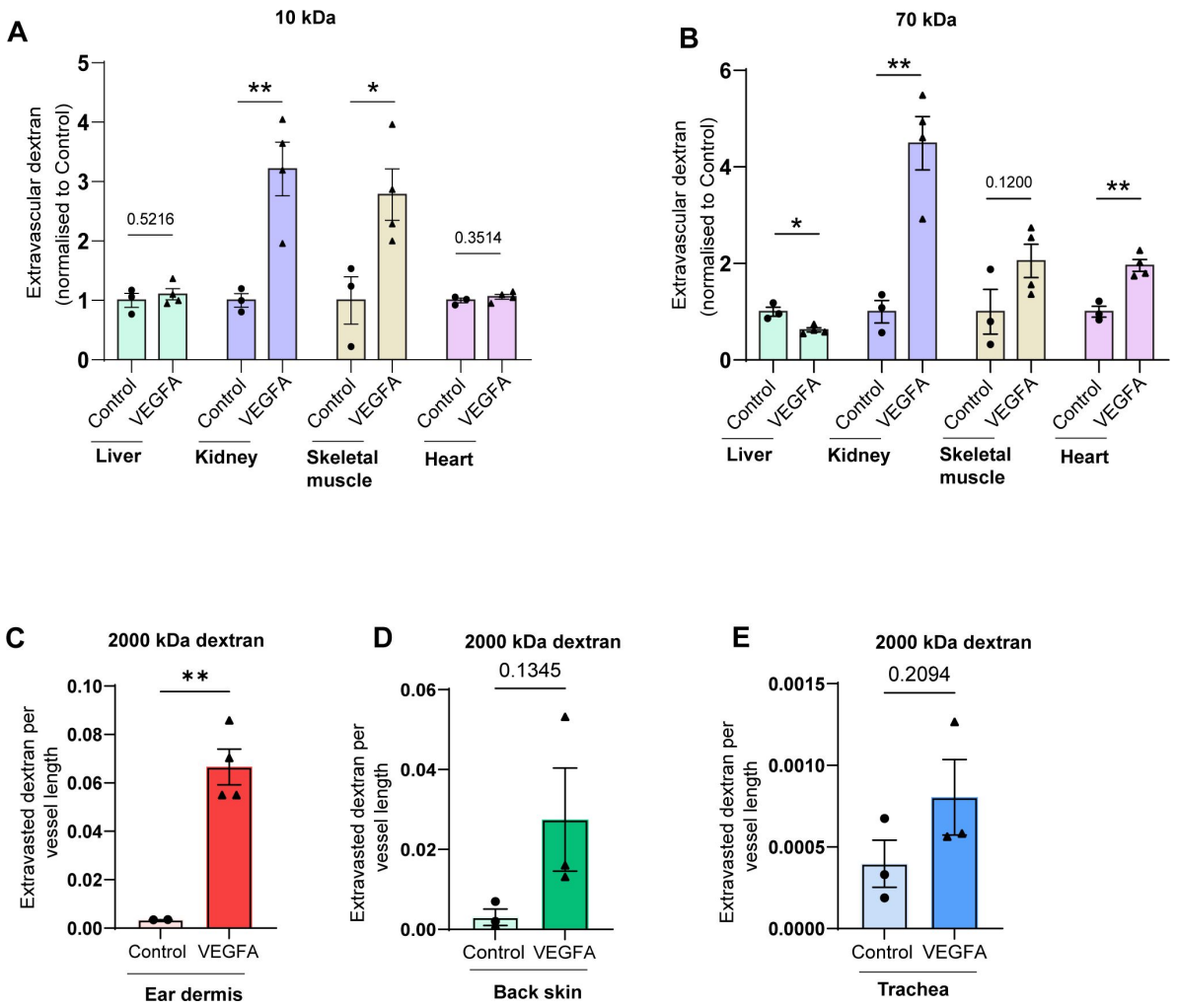

Supplementary Figure 2.

Organotypic assessment of VEGFA-induced leakage

(A,B) Leakage of 10 kDa **(A)** and 70 kDa **(B)** dextran after systemic administration of only dextran (control) and dextran plus VEGFA in liver, kidney, skeletal muscle and heart of wild-type C57Bl/6 mice (n ≥ 3 mice).
(C-E) Leakage of 2000 kDa dextran after systemic administration of only dextran (control) and dextran plus VEGFA in ear dermis **(C)**, back skin **(D)** and trachea **(E)** of wild-type C57Bl/6 mice (n ≥ 2 mice).
Error bars; mean ± SEM. Statistical significance used: Two-tailed unpaired student's t-test

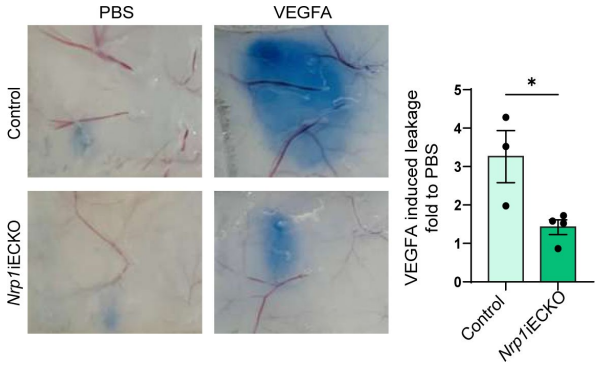

Supplementary Figure 3.

Loss of EC NRP1 reduces VEGFA mediated vascular permeability in the back skin

Evans blue leakage with intradermal administration of VEGFA in the back skin of *Nrp1* iECKO mice. Left, representative images. Right, quantification of Evans blue extravasation shown as VEGFA induced leakage fold over PBS (n ≥ 3 mice). Error bars; mean ± SEM. Statistical significance used: Two-tailed unpaired student's t-tes

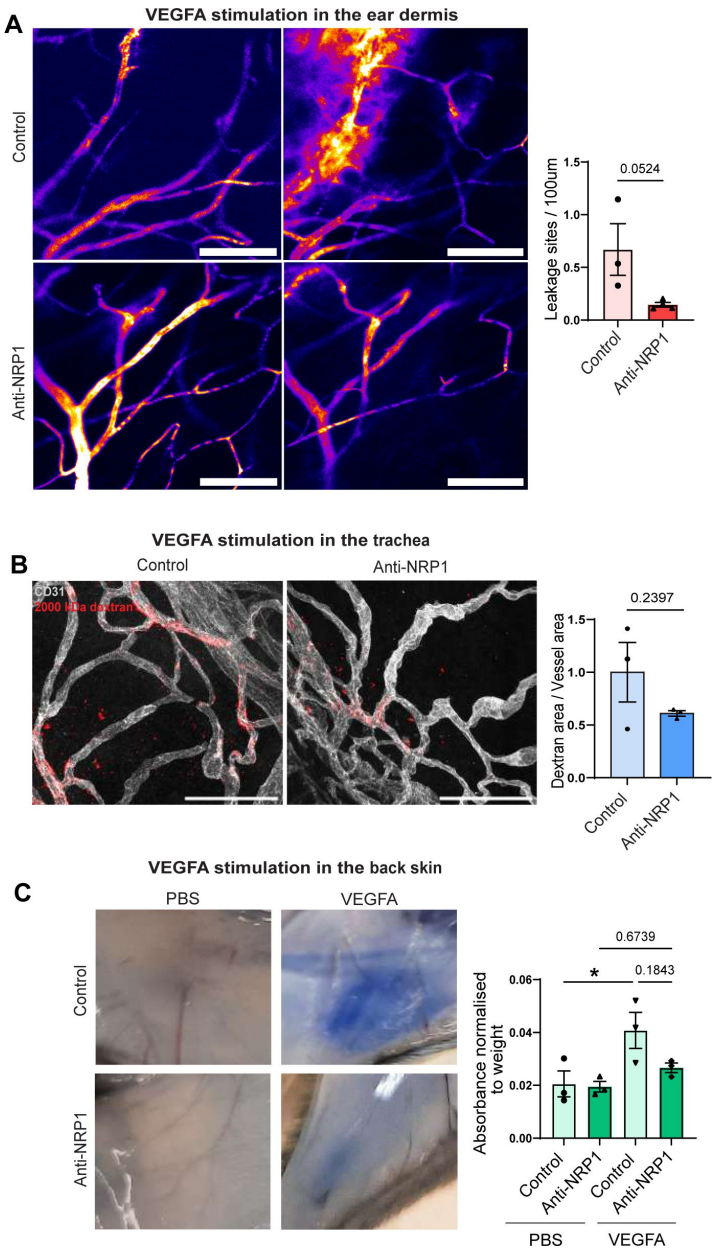

Supplementary figure 4.

Global inactivation of NRP1 reduces VEGFA mediated vascular permeability

(A) VEGFA-induced leakage in the ear skin of C57Bl/6 mice treated intradermally with isotype control or NRP1 blocking antibody. Left, representative images. Right, quantification of leakage sites per 100 µm of vessel length (n=3 mice, 3 acquisitions/mouse).
(B) Leakage of 2000 kDa dextran in trachea of C57Bl/6 mice treated systemically with isotype control or NRP1 blocking antibody. Left, representative images. Right, quantification of tracer area/vessel area (n=3 mice).
(C) PBS and VEGFA-induced leakage in the back skin of C57Bl/6 mice treated intradermally with isotype control or NRP1 blocking antibody. Left, representative images. Right, quantification of Evans blue leakage (n=3 mice).
Error bars; mean ± SEM. Statistical significance used: Two-tailed unpaired student's t-test. Scale bar: 100µm

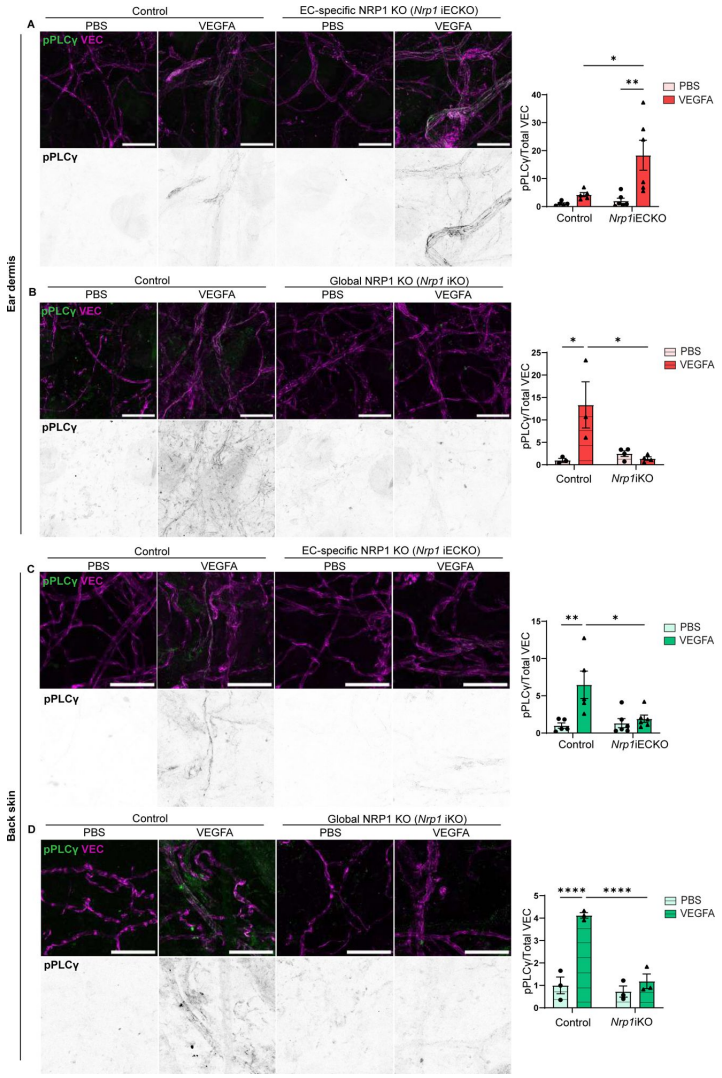

Supplementary figure 5.

Perivascular NRP1 modifies PLCγ phosphorylation

(A-B) Phosphorylation of PLCγ in response to intradermal PBS or VEGFA injections in the ear dermis of control and *Nrp1* iECKO (A) or *Nrp1* iKO (B) mice. Left, representative images. Right, quantification of phosphorylated PLCγ area per total VEC area normalized to PBS control in the ear dermis of control and *Nrp1* iECKO or *Nrp1* iKO mice. n≥3 mice, two or more fields of view/mouse.
(C-D) Phosphorylation of PLCγ in response to intradermal PBS or VEGFA injections in the back skin of control and *Nrp1* iECKO (C) or *Nrp1* iKO (D) mice. Left, representative images. Right, quantification of phosphorylated PLCγ area per total VEC area normalized to PBS control in the back skin of control and *Nrp1* iECKO or *Nrp1* iKO mice. n≥3 mice, two or more fields of view/mouse.
Error bars; mean ± SEM. Statistical significance: Two-way ANOVA. Scale bar: 50μm

References

Acevedo L. M., Barillas S., Weis S. M., Göthert J. R., Cheresh D. A (2008) **Semaphorin 3A suppresses VEGF-mediated angiogenesis yet acts as a vascular permeability factor** *Blood* **111**:2674–80

Aird W. C (2007) **Phenotypic heterogeneity of the endothelium: I. Structure, function, and mechanisms** *Circ Res* **100**:158–73

Augustin H. G., Koh G. Y (2017) **Organotypic vasculature: From descriptive heterogeneity to functional pathophysiology** *Science* **357**

Ballmer-Hofer K., Andersson A. E., Ratcliffe L. E., Berger P (2011) **Neuropilin-1 promotes VEGFR-2 trafficking through Rab11 vesicles thereby specifying signal output** *Blood* **118**:816–26

Bartlett C. S., Scott R. P., Carota I. A., Wnuk M. L., Kanwar Y. S., Miner J. H., Quaggin S. E (2017) **Glomerular mesangial cell recruitment and function require the co-receptor neuropilin-1** *Am J Physiol Renal Physiol* **313**:F1232–F1242

Bayliss A. L., Sundararaman A., Granet C., Mellor H (2020) **Raftlin is recruited by neuropilin-1 to the activated VEGFR2 complex to control proangiogenic signaling** *Angiogenesis* **23**:371–383

Becker P. M., Waltenberger J., Yachechko R., Mirzapoiazova T., Sham J. S., Lee C. G., Elias J. A., Verin A. D (2005) **Neuropilin-1 regulates vascular endothelial growth factor-mediated endothelial permeability** *Circ Res* **96**:1257–65

Bosseboeuf E. *et al.* (2023) **Neuropilin-1 interacts with VE-cadherin and TGFBR2 to stabilize adherens junctions and prevent activation of endothelium under flow** *Sci Signal* **16**

Cai H., Reed R. R (1999) **Cloning and characterization of neuropilin-1-interacting protein: a PSD-95/Dlg/ZO-1 domain-containing protein that interacts with the cytoplasmic domain of neuropilin-1** *J Neurosci* **19**:6519–27

Cerani A. *et al.* (2013) **Neuron-derived semaphorin 3A is an early inducer of vascular permeability in diabetic retinopathy via neuropilin-1** *Cell Metab* **18**:505–18

Corti F., Ristori E., Rivera-Molina F., Toomre D., Zhang J., Mihailovic J., Zhuang Z. W., Simons M. (2022) **Syndecan-2 selectively regulates VEGF-induced vascular permeability** *Nature Cardiovascular Research* **1**:518–528

Fantin A. *et al.* (2017) **VEGF165-induced vascular permeability requires NRP1 for ABL-mediated SRC family kinase activation** *J Exp Med* **214**:1049–1064

Fernández-Robredo P., Selvam S., Powner M. B., Sim D. A., Fruttiger M (2017) **Neuropilin 1 Involvement in Choroidal and Retinal Neovascularisation** *PLoS One* **12**

Gioelli N. *et al.* (2022) **Neuropilin 1 and its inhibitory ligand mini-tryptophanyl-tRNA synthetase inversely regulate VE-cadherin turnover and vascular permeability** *Nat Commun* **13**

Goshima Y. *et al.* (1999) **Growth cone neuropilin-1 mediates collapsin-1/Sema III facilitation of antero- and retrograde axoplasmic transport** *J Neurobiol* **39**:579–89

Gu C., Limberg B. J., Whitaker G. B., Perman B., Leahy D. J., Rosenbaum J. S., Ginty D. D., Kolodkin A. L (2002) **Characterization of neuropilin-1 structural features that confer binding to semaphorin 3A and vascular endothelial growth factor 165** *J Biol Chem* **277**:18069–76

Hong T. M. *et al.* (2007) **Targeting neuropilin 1 as an antitumor strategy in lung cancer** *Clin Cancer Res* **13**:4759–68

Honkura N., Richards M., Lavina B., Sainz-Jaspeado M., Betsholtz C., Claesson-Welsh L. (2018) **Intravital imaging-based analysis tools for vessel identification and assessment of concurrent dynamic vascular events** *Nat Commun* **9**

Horowitz A., Seerapu H. R (2012) **Regulation of VEGF signaling by membrane traffic** *Cell Signal* **24**:1810–20

Hu B., Guo P., Bar-Joseph I., Imanishi Y., Jarzynka M. J., Bogler O., Mikkelsen T., Hirose T., Nishikawa R., Cheng S. Y. (2007) **Neuropilin-1 promotes human glioma progression through potentiating the activity of the HGF/SF autocrine pathway** *Oncogene* **26**:5577–86

Jin Y. *et al.* (2022) **Tyrosine-protein kinase Yes controls endothelial junctional plasticity and barrier integrity by regulating VE-cadherin phosphorylation and endocytosis** *Nature Cardiovascular Research* **1**:1156–1173

Jung B., Arnold T. D., Raschperger E., Gaengel K., Betsholtz C (2018) **Visualization of vascular mural cells in developing brain using genetically labeled transgenic reporter mice** *J Cereb Blood Flow Metab* **38**:456–468

Kawakami T., Tokunaga T., Hatanaka H., Kijima H., Yamazaki H., Abe Y., Osamura Y., Inoue H., Ueyama Y., Nakamura M (2002) **Neuropilin 1 and neuropilin 2 co-expression is significantly correlated with increased vascularity and poor prognosis in nonsmall cell lung carcinoma** *Cancer* **95**:2196–201

Kawasaki T., Kitsukawa T., Bekku Y., Matsuda Y., Sanbo M., Yagi T., Fujisawa H (1999) **A requirement for neuropilin-1 in embryonic vessel formation** *Development* **126**:4895–902

Kitsukawa T., Shimono A., Kawakami A., Kondoh H., Fujisawa H (1995) **Overexpression of a membrane protein, neuropilin, in chimeric mice causes anomalies in the cardiovascular system, nervous system and limbs** *Development* **121**:4309–18

Koch S., Van Meeteren L. A., Morin E., Testini C., Weström S., Björkelund H., Le Jan S., Adler J., Berger P., Claesson-Welsh L. (2014) **NRP1 presented in trans to the endothelium arrests VEGFR2 endocytosis, preventing angiogenic signaling and tumor initiation** *Dev Cell* **28**:633–46

Lanahan A. *et al.* (2013) **The neuropilin 1 cytoplasmic domain is required for VEGF-A-dependent arteriogenesis** *Dev Cell* **25**:156–68

Lanahan A. A., Hermans K., Claes F., Kerley-Hamilton J. S., Zhuang Z. W., Giordano F. J., Carmeliet P., Simons M (2010) **VEGF receptor 2 endocytic trafficking regulates arterial morphogenesis** *Dev Cell* **18**:713–24

Li X. *et al.* (2016) **VEGFR2 pY949 signalling regulates adherens junction integrity and metastatic spread** *Nat Commun* **7**

Mamluk R., Gechtman Z., Kutcher M. E., Gasiunas N., Gallagher J., Klagsbrun M (2002) **Neuropilin-1 binds vascular endothelial growth factor 165, placenta growth factor-2, and heparin via its b1b2 domain** *J Biol Chem* **277**:24818–25

Matsumoto T. *et al.* (2005) **VEGF receptor-2 Y951 signaling and a role for the adapter molecule TSAd in tumor angiogenesis** *Embo j* **24**:2342–53

Mcgowan S. E., Mccoy D. M (2021) **Neuropilin-1 directs PDGFRalpha-entry into lung fibroblasts and signaling from very early endosomes** *Am J Physiol Lung Cell Mol Physiol* **320**:L179–L192

Miao H. Q., Lee P., Lin H., Soker S., Klagsbrun M (2000) **Neuropilin-1 expression by tumor cells promotes tumor angiogenesis and progression** *FASEB J* **14**:2532–9

Morin E., Lindskog C., Johansson M., Egevad L., Sandström P., Harmenberg U., Claesson-Welsh L., Sjöberg E (2020) **Perivascular Neuropilin-1 expression is an independent marker of improved survival in renal cell carcinoma** *The Journal of Pathology* **250**:387–396

Morin E. *et al.* (2018) **VEGF receptor-2/neuropilin 1 trans-complex formation between endothelial and tumor cells is an independent predictor of pancreatic cancer survival** *The Journal of Pathology* **246**:311–322

Naccache S. N., Hasson T., Horowitz A (2006) **Binding of internalized receptors to the PDZ domain of GIPC/synectin recruits myosin VI to endocytic vesicles** *Proc Natl Acad Sci U S A* **103**:12735–40

Orsenigo F. *et al.* (2012) **Phosphorylation of VE-cadherin is modulated by haemodynamic forces and contributes to the regulation of vascular permeability in vivo** *Nat Commun* **3**

Pan Q. *et al.* (2007) **Blocking neuropilin-1 function has an additive effect with anti-VEGF to inhibit tumor growth** *Cancer Cell* **11**:53–67

Ponuwei G. A (2016) **A glimpse of the ERM proteins** *J Biomed Sci* **23**

Raimondi C., Fantin A., Lampropoulou A., Denti L., Chikh A., Ruhrberg C (2014) **Imatinib inhibits VEGF-independent angiogenesis by targeting neuropilin 1-dependent ABL1 activation in endothelial cells** *J Exp Med* **211**:1167–83

Richards M. *et al.* (2022) **Claudin5 protects the peripheral endothelial barrier in an organ and vessel-type-specific manner** *Elife* **11**

Richards M., Pal S., Sjöberg E., Martinsson P., Venkatraman L., Claesson-Welsh L (2021) **Intra-vessel heterogeneity establishes enhanced sites of macromolecular leakage downstream of laminin α5** *Cell Rep* **35**

Roth L., Prahst C., Ruckdeschel T., Savant S., Weström S., Fantin A., Riedel M., Héroult M., Ruhrberg C., Augustin H. G (2016) **Neuropilin-1 mediates vascular permeability independently of vascular endothelial growth factor receptor-2 activation** *Sci Signal* **9**

Sarris M., Andersen K. G., Randow F., Mayr L., Betz A. G (2008) **Neuropilin-1 expression on regulatory T cells enhances their interactions with dendritic cells during antigen recognition** *Immunity* **28**:402–13

Shahrabi-Farahani S., Gallottini M., Martins F., Li E., Mudge D. R., Nakayama H., Hida K., Panigrahy D., D'amore P. A., Bielenberg D. R (2016) **Neuropilin 1 Receptor Is Up-Regulated in Dysplastic Epithelium and Oral Squamous Cell Carcinoma** *Am J Pathol* **186**:1055–64

Sherafat A., Pfeiffer F., Reiss A. M., Wood W. M., Nishiyama A (2021) **Microglial neuropilin-1 promotes oligodendrocyte expansion during development and remyelination by trans-activating platelet-derived growth factor receptor** *Nat Commun* **12**

Sjoberg E. *et al.* (2023) **Endothelial VEGFR2-PLCgamma signaling regulates vascular permeability and antitumor immunity through eNOS/Src** *J Clin Invest* **133**

Soker S., Miao H. Q., Nomi M., Takashima S., Klagsbrun M (2002) **VEGF165 mediates formation of complexes containing VEGFR-2 and neuropilin-1 that enhance VEGF165-receptor binding** *J Cell Biochem* **85**:357–68

Sun Z. *et al.* (2012) **VEGFR2 induces c-Src signaling and vascular permeability in vivo via the adaptor protein TSAd** *J Exp Med* **209**:1363–77

Wang J., Wang S., Li M., Wu D., Liu F., Yang R., Ji S., Ji A., Li Y (2015) **The Neuropilin-1 Inhibitor, ATWLPPR Peptide, Prevents Experimental Diabetes-Induced Retinal Injury by Preserving Vascular Integrity and Decreasing Oxidative Stress** *PLoS One* **10**

Wessel F. *et al.* (2014) **Leukocyte extravasation and vascular permeability are each controlled in vivo by different tyrosine residues of VE-cadherin** *Nat Immunol* **15**:223–30

Wnuk M., Anderegg M. A., Graber W. A., Buergy R., Fuster D. G., Djonov V (2017) **Neuropilin1 regulates glomerular function and basement membrane composition through pericytes in the mouse kidney** *Kidney Int* **91**:868–879

Article and author information

Sagnik Pal

Dept. of Immunology, Genetics and Pathology, Beijer and Science for Life Laboratories, Uppsala University, Uppsala, Sweden
ORCID iD: 0000-0002-5562-1555

Yangyang Su

Dept. of Immunology, Genetics and Pathology, Beijer and Science for Life Laboratories, Uppsala University, Uppsala, Sweden

Lena Claesson-Welsh

Dept. of Immunology, Genetics and Pathology, Beijer and Science for Life Laboratories, Uppsala University, Uppsala, Sweden
ORCID iD: 0000-0003-4275-2000

Mark Richards
Dept. of Immunology, Genetics and Pathology, Beijer and Science for Life Laboratories, Uppsala University, Uppsala, Sweden
For correspondence: mark.richards@igp.uu.se
ORCID iD: 0000-0002-2266-3329

Copyright

Editors

Reviewing Editor
Dietmar Vestweber
Max Planck Institute for Molecular Biomedicine, Münster, Germany

Senior Editor
Didier Stainier
Max Planck Institute for Heart and Lung Research, Bad Nauheim, Germany

Reviewer #1 (Public Review):

Summary:

This study examines how blood vessels exposed to the cytokine VEGF respond to vascular leakage when the VEGF receptor NRP1 is targeted. This study compares results in in two different body sites of the dermis and in a different organ, the trachea. The authors refer to the two different sites of the dermis as two different organs, but the dermis is one organ. The authors report that vascular leakage is differentially affected by NRP1 targeting in the ear skin compared to the trachea and back skin. They attribute these differences to NRP1 presence in cells other than the vascular endothelium, especially in the ear skin, where they observe higher perivascular NRP1 staining.

The manuscript states that the aim was to uncover the role of NRP1 in VEGF-mediated vascular permeability. This was misleading, because a lot is already known on NRP1 in this pathway, as is evidenced by a large number of publications the authors themselves quote (and sometimes misquote). The main information they wish to add is the possibility that NRP1 may also play a role in other cells to regulate permeability, as they previously suggested for blood vessel growth. Several technical issues and experimental limitations call into question whether the above conclusion can be reached with the data provided.

Strengths:

It is an interesting concept that NRP1 regulates vascular permeability by acting in perivascular cells.

Weaknesses:

(A) Technical limitations due to assay type:

A direct comparison of the skin in two body sites is not warranted given that the authors used different methods to study the two sites. Below is a list of differences reported in their methods section:

(A1) Different tracers were used to visualize VEGF165-induced leakage in different sites.
Ear skin assay: 2 kDa FITC and two different dextrans, 10 kDa TRITC dextran, and another dextran whose molecular weight is not specified. It is not explained why 3 different tracers were used. Figures 1 and 2 report data with 2 kDa TRITC dextran.
Back skin assay: They describe the Miles assay using Evans Blue, which binds to albumin, making it a 67 kDa tracer. However, Figure 1 suggests that 2 kDa dextran was used, and perhaps Evans Blue was only used for the supplemental data. This is relevant because current knowledge suggests that small dyes use the junctional pathway, whereas larger proteins such as albumin can use vesicular transport. The former is thought to be a fast pathway (hence, the authors measured dye extravasation 3 min after VEGF165 injection). The latter pathway is a slower one (hence, measured 30 min after VEGF165 injection in the Miles assay).

Quantification: For ear skin, the number of leakage sites and lag period is quantified, as well as leakage over time. For back skin, the amount of extravasated dye is quantified at a fixed time point. Such different measurements do not allow for direct comparison.

(A2) Mice were prepared in different ways for the different body sites studied:
Ear skin assay: general anesthesia with ketamine-xylazine.
Back skin assay: No anesthesia is described for the back skin Miles assay. This would be a concern because intradermal injections are considered to be painful. For back skin histology, they do report to have used isoflurane anesthesia before perfusion fixation. However, it is not advisable to use used isoflurane anesthesia for perfusion fixation if this has been done via the conventional cardiac route, because opening the chest cavity to access the heart for perfusion causes lung collapse, meaning that the mice cannot breathe the anaesthetic, and there is a risk of them regaining consciousness. The authors should clarify what exactly they have done, for ethical reasons and also because the type of anesthesia can affect vascular studies, for example, see PMID 36418078.

(A3) Differential histamine use:
Back skin assay: uses anti-histamine, as is advised with intradermal injections to minimize vascular leakage due to histamine release after local trauma.
Ear skin assay: no anti-histamine was used, so histamine-induced background leakage might have been present, independently of VEGF165. The authors suggest that the ear skin injection does not cause trauma, but it is unclear how this is possible, given that skin needs to be disrupted for the needle to enter the tissue.

(A4) Different VEGF165 concentration used:
The ear skin assay uses 10 ng VEGF per injection, and the back skin assay 80 ng.

Given all these differences in experimental protocols, as well as different knockdown efficiency (see below), the results for the different sites are not directly comparable. Hence it cannot presently be concluded that the role of NRP1 in both sites is different, and further work is required to make a firm conclusion. In addition, the conflicts between the reported methods and figures need to be resolved.

(B) It is unclear whether appropriate controls were used:

(B1) What genotype and treatment are the control mice for NRP1 targeting? The ideal control would be wild-type mice with the same CreER, injected with tamoxifen according to the same timeline, to account for vehicle, tamoxifen, and tamoxifen-induced CreER toxicity (https://doi.org/10.1038/s44161-022-00125-6). This could be a littermate mouse or, alternatively, a

separate experiment should be shown comparing wild-type mice carrying the same CreER as used for the ablation studies and injected with tamoxifen, versus wild-type mice injected with tamoxifen, to demonstrate that the induction regime does not in itself cause phenotypes.

(B2) Has a PBS injection been performed to compare baseline leakage between genotypes, independently of VEGF165 injections? This is an essential control.

(B3) The experimental protocol assays 4 days after 5 consecutive tamoxifen injections, which does not allow much time for drug washout. Moreover, this is a lot of tamoxifen (80 mg x 5 = 400 mg tamoxifen per kg). Due to the possibility that tamoxifen-induced effects might still be present and cause sex-differential effects, the corresponding sex for each individual data point should be indicated in all graphs.

(B4) i.p. peanut oil is used in undefined volumes; this vehicle was shown to cause inflammation if administered i.p. (PMID 33139505). Therefore, inflammation might be present, which might affect different body sites differently.

(C) Validation of NRP1 targeting:
The authors have not performed an NRP1 knockout in the endothelium, as they repeatedly claim. In the lung, there is a good knockdown of around 75%; this may or may not be due to complete EC knockdown with preservation of NRP1 in other cell types. In the trachea, ear skin, and back skin, knockdown was not quantified, although qualitative comparisons by NRP1 immunostaining in Supplementary Figure 1 suggest that the back skin targeting worked better than the ear skin targeting, which would confound results, but in any case, it was neither a knockdown nor knockout. The staining for global targeting looks fainter than for the other genotypes, and the single-channel images seem to have different intensities than the overlays in Supplementary Figure 1 A.

(D) Systemic permeability studies:
Organs have very different baseline permeability, due to the properties of the vascular barrier, i.e. tight barriers in the brain and retina and permeable endothelium in the liver and kidney. In this assay, VEGF is not delivered from the tissue side, as would be typical during inflammation but is delivered through the circulation, which has been shown to differentially affect the VEGF response, at least in some tissues (PMID 25175707). Nevertheless, this is a helpful readout, especially given that PBS controls appear not to have been performed above to establish baseline leakage between genotypes and tissues.

Figure Supplement 3 shows that VEGF induces vascular leakage in all body sites examined, independently of the size of the tracer used, and agreeing with current literature. An additional set of panels should be included with data shown without calculating the fold change relative to the control, set to 1, to account for the endothelium in different organs having different baseline vascular permeability. How do the authors explain that VEGF has the same effect in the ear and back skin in this assay, when NRP1 is present, given that they claim a role for perivascular NRP1 in the ear, but not back skin, for reducing VEGF/VEGFR2 signalling?

(E) Comparing results obtained with different tools:

- The endothelial NRP1 knockdown yielded different results for ear and back skin.
- Anti-NRP1 yielded similar results for ear and back skin.
- The global NRP1 ko yielded similar results for ear and back skin.

Because anti-NRP1 and the global NRP1 knockdown gives similar results for all tissues, the authors deduce that the NRP1 acts in cell types other than endothelial cells to regulate permeability. This is an interesting idea, based on the lab's prior work in angiogenesis. In their trans-interaction scenario, NRP1 would have the same role in ECs in all sites, but non-endothelial NRP1 can override the function of the endothelial NRP1 function depending on its expression levels.

Confidence in this conclusion would require additional experiments:
- Show that the endothelial knockdown works equally well in different body sites, via NRP1 staining and/or by checking recombination efficiency with a reporter.
- Using an analogous assay to measure permeability in different body sites.
- Perform a non-endothelial knockdown, i.e. in pericytes, which is hypothesized to be the source of NRP1 that affects vascular leakage signalling in endothelial cells in trans.

(F) Abstract, introduction, and references:
The authors suggest controversy with regard to NRP1's roles in permeability. However, NRP1's function in VEGF signalling has been defined as being an accessory to VEGFR2, with a role in promoting SFK activation. This function relies on the NRP1 cytoplasmic domain, which mediates VEGFR2 trafficking and signalling; the relevant literature for the NRP1 cytoplasmic domain is mentioned for arteriogenesis (PMID 23639442), but not permeability (PMID 28289053). Another paper is mentioned which describes a VEGFR2-independent pathway for a CendR ligand, but this prior study did NOT make the claim that VEGF signalling is NRP1-independent or promotes it (PMID 27117252). In the eye, NRP1 has been implicated in both SEMA3A and VEGF165-induced permeability, which was also corroborated by the Miles assay in two prior studies (PMID 18180379, PMID 28289053). The last sentence in the abstract is incorrect, because differences in ear versus back skin do not constitute organotypic difference (as the organ is the dermis), and the potential role of perivascular cells is only inferred from the global endothelial NRP1 knockdown, which gives the same result as reported for the endothelial NRP1 knockdown in the literature.

(1) Lines 5/.53: The references for VEGF-NRP1 signalling in age-related macular degeneration are not helpful: Raimondi investigated VEGF-independent NRP1 pathways in angiogenesis, Fernandez-Robredo investigated NRP1 pathways in angiogenesis and showed that fewer vessels correlated with less leakage but did not test VEGF signaling specifically. A more suitable reference would have been PMID 28289053.

(2) Lines 63/64 and repeated in 84-89: The references quoted all showed that NRP1 inhibition reduces vascular permeability, and therefore do not provide evidence for the idea that NRP1 inhibition promotes permeability, as the authors report here for the ear skin; the only study supporting them is one using arterial endothelial cells, which are not permeability-relevant.

(3) Lines 106/107: The references used to underpin organ-specific barrier properties are correct, but as stated above, the dermis is the dermis, and therefore, these references would not be useful to provide support for the idea that the ear and back skin behave differently after NRP1 knockdown.

(G) Additional comments on the figures:
Figure 4: The authors show that VEGFR2 is essential for permeability, and VEGF164 effects are VEGFR2 dependent - this is well established for VEGF164 in the Miles assay, including the accessory role of NRP1 (e.g. PMID 28289053). As the proposed trans function of NRP1 cannot make a difference in VEGFR2 signaling when VEGFR2 is not there, this experiment is only confirmatory of prior VEGFR2 knowledge.

https://doi.org/10.7554/eLife.95934.1.sa2

Reviewer #2 (Public Review):

The paper by Pal et al. examines the role of Nrp1 in organ-specific permeability response to VEGF. The subject is certainly interesting, but there are a number of significant methodological problems that make data evaluation rather problematic. In particular, lung endothelial cells are used to assess the effectiveness of Nrp1 knockout when experiments

focus on different organs; small number of data points (as small as 2 or 3) are used to claim statistically significant differences; obvious data scatter is not commented on and seems ignored; key reagents (anti-Nrp1 Ab) are not well characterized, a proposed model is not verified in vitro, etc. Some of these issues are outlined in detail below, but the list of problems is much longer than this.

(1) Intradermal injection of anti-Nrp1 Ab: I am puzzled by this experiment: Will Ab presence be limited locally or is there a systemic distribution? This needs to be verified.

(2) What does anti-Nrp1 Ab actually do? Does it block VEGF binding? Induces Nrp1 and VEGFR2 endocytosis?

(3) How does i.v. injection of anti-Nrp1 Ab affect permeability in different organs?

(4) Effect of endothelial Nrp1KO: Since the authors examine organ-specific effects of Nrp1, it seems illogical to assess its expression in the lung as a measure of KO as KO efficiency may differ organ by organ. Immunocytochemistry is not particularly quantitative and prone to selection bias. I'd suggest using EC bulk RNAseq from different organs to confirm the magnitude of the knockout in different beds.

(5) Figures 1B and 2B show profoundly different levels of Nrp1 KO in lung ECs. Were different mouse strains used in Figure 1 and Figure 2 experiments? This may well explain the differences the authors have observed.

(6) Supplementary Figure 2: why is there no leakage of 10kD dextran in the heart in response to VEGF when there is an increase in the 70kD dextran leakage? That does not seem possible. Further, the authors observed no significant increase in 70kD dextran leakage after VEGF in the skeletal muscle. That also seems very unlikely and flies against experience of many labs in the field.

(7) Since the authors think that peri-vascular cell Nrp1 expression accounts for organ-specific Nrp1 effects, this should be studied and examined in an in vitro co-culture model.

(8) Quantification: a lot of quantifications- of Nrp1 expression level, VE-cadherin Y685 phosphorylation, etc. are done on the basis of immunocytochemistry. This really is not a quantitative technique and is prone to numerous artifacts. The data should be at least confirmed by whole-tissue Westerns. I am also puzzled by small numbers of samples. If each dot on a graph represents an individual data point, how do authors get a $p<0.5$ value with an N of 3? (for example Figure 5B, but there are other examples). Also, in Figure 4F data scatter is quite enormous. This is either an experimental problem or, more likely, there is a biological message here - the tissue is not uniform. In any case, I do not see how one gets a significant result here. Figures 5B and 5C have a similar problem while Figure 5D seems to be based on only two data points?

https://doi.org/10.7554/eLife.95934.1.sa1

Reviewer #3 (Public Review):

Summary:

Pal et al. provide valuable evidence supporting distinct vascular bed-specific VEGF-A mediated vascular permeability function of Neuropilin-1 (NRP1) in adult mice. Using a suite of genetic mice models and state-of-the-art vascular permeability assays the authors demonstrate that ear skin vasculature of EC-specific NRP1 adult knockout mice is hypersensitive to VEGF-A mediated high-molecular weight dye leakage from venules, as opposed to back skin and tracheal vasculature where EC-specific NRP1 loss had a more

classical negative effect on permeability. Interestingly, both whole organism KO of NRP1 and a blocking antibody treatment, attenuated VEGF-A mediated permeability in ear skin and had the usual attenuation of permeability phenotype in back skin and tracheal vasculature. Using a pericyte promoter specific reporter mice line, the authors characterize NRP1 expression in the vascular beds of the ear dermis and back skin and conclude that NRP1 expression is higher in perivascular cells in the ear dermis as opposed to back skin vasculature, thus indicating a juxtracrine NRP1-VEGFR2 signaling model in adult mice. Further, they use a Vegfr2 phosphosite mutant homozygous mice model in the background of NRP1 iECKO to find the hypersensitivity to VEGF-A stimulation in ear skin is abrogated and therefore, prove the juxtracrine NRP1 control of VEGFR2 mediated downstream signaling leading to vascular permeability. Further, they successfully show distinctive vascular bed-specific results as above using a well-characterized VE-Cadherin Y685 antibody staining which corresponds to vascular leakage downstream of VEGF-A/VEGFR2 signaling in ear dermis and back skin vascular beds.

Strengths:

The question of the in vivo role of NRP1 in VEGF-A-induced hyper-permeability is an unresolved one and the elegant use of genetic mice models to demonstrate the phenotypes is valuable to the field. The organotypic differences observed in vascular permeability upon VEGF-A treatment in ear skin versus back skin and tracheal vasculature are solid. The subsequent investigation to validate heightened VEGFR2 signaling in ear dermis downstream of VEGF-A stimulation using Vegfr2 Y949F mice, VEC Y685 antibody, and pPLCγ antibody is also very convincing.

Weaknesses:

The mechanism proposed by the authors by which EC-specific loss of NRP1 caused hypersensitivity to VEGF-A in ear dermis is through elevated juxtracrine signaling of NRP1 expressed in pericytes in trans binding and retaining VEGFR2 on the cell surface of ECs to sustain downstream signaling for longer time, in corroboration to earlier findings in Koch et al., 2014, where NRP1 was studied in the context of tumor angiogenesis. To support their claim, the authors stain the ear dermis and back skin vasculature of Pdgfrb-GFP reporter mice, with NRP1 and CD31 antibodies and find out that ear skin vasculature has higher perivascular cells as opposed to back skin vasculature. While this is a good experiment to prove the above point, there are no functional experiments to support this model.

Overall, although the paper presents very useful findings in the field of NRP1-VEGFR2 biology, and most of the conclusions are well supported by the data, there are a few points if addressed can significantly substantiate the model of juxtracrine signaling proposed by the authors. They are:

(1) It will be important to know if the perivascular to vascular NRP1 expression (such as in Figure 3B) increases further in ear skin vasculatures of NRP1 iECKO mice compared to otherwise WT mice.

(2) Does knocking out NRP1 in pericytes attenuate the VEGF-A mediated hyperpermeability observed in ear skin of NRP1 iECKO mice (similar to experiments in 1C, 2C)?

(3) What is the status of VEGFR2 expression in ECs of ear skin and back skin of NRP1 iECKO and NRP1 iKO mice? This experiment is a proof-of-concept and is not essential to prove the point of juxtracrine NRP1 signaling since downstream readouts - pPLCγ and VEC Y685 staining have already been shown to correlate in the ear dermis.

https://doi.org/10.7554/eLife.95934.1.sa0